A Formula for the Total Longshore Sediment Transport Rate
- Development and Evaluation -

By

Mushaliza Mustar

Department of Water Resources Engineering
Lund Institute of Technology/Lund University
Lund, Sweden
LU:2005:19

Preface

I would like to take this opportunity to thank the following persons:

- The Lord of Almighty for His bless, giving me the chances to learn and to finish this report.

- Dr. Koos Schoonees for his kindness in providing me with his extensive longshore transport data base, and for valuable explanations.

- Dr. Atilla Bayram for providing longshore transport data, together with valuable explanations.

- Professor Magnus Larson for introducing me to the topic, explaining many problems regarding the subject, guiding and assisting me with the analysis, and many valuable discussions.

- JPA and USM (as an organisation) in Malaysia for giving me the opportunity to extend my knowledge.

I would also like to dedicate my work to my beloved family and my husband with all my heart. They have always been there for me, filled my days with their love and support.

Last but not least, to my Swedish friends: Sabina, Linnea, and Karin - thanks for your kindness, love, and support throughout the years.

Professor Magnus Larson, Department of Water Resources Engineering, acted as supervisor for this study.

ABSTRACT

Title: A formula for the total longshore sediment transport rate
- Development and evaluation –

Author: Mushaliza Mustar

Supervisor: Prof. Magnus Larson, Department of Water Resources Engineering, Lund University, Lund, Sweden.

Presentation of problem: The movement of sediment parallel to the coast by waves and currents is known as longshore sediment transport or littoral transport. Throughout the years, researchers have found that knowledge of longshore sediment transport is important in connection with coastal engineering design, such as construction of breakwaters at harbour entrances, dredging of navigation channels, and improving beaches. During the last three decades, a number of different longshore transport formulas have been proposed. These formulas were based on different approaches, such as the energetic or energy flux approach, the shear stress or modified steady flow approach, as well as others.

Objectives: The main objectives of this study are:

(a) to develop a formula for the total longshore sediment transport

(b) to evaluate the newly developed formula for the longshore sediment transport by comparison with an extensive, high-quality field and laboratory data base

(c) to determine values on the empirical coefficient appearing in the new formula

Procedure: This study was conducted as follows:

(a) literature on longshore sediment transport was reviewed

(b) a formula for the longshore sediment transport was developed based on the formulation proposed by Larson and Bayram (2005)

(c) an extensive data base on longshore sediment transport rates was compiled from the literature, encompassing both laboratory and field data

(d) values on an empirical coefficient appearing in the new formula were evaluate and validated

Conclusions: In general, based on the calculation results, the newly developed formula yielded overall good predictions. The pattern in the graph which compares measured and calculated transport rates for all data sets is similar, although a few points that are located far away from the main group of points. The calculated empirical coefficient is in the range between 0.00018 and 0.0052, whereas the calculated standard deviation ranged from 0.0001 to 0.0024. It is likely that some additional factors influence the value of the empirical coefficient and an analysis was performed to relate the coefficient value to various quantities, such as fall velocity, deep water wave height, wavelength, grain size, and wave period. In conclusion, the objectives in this report, which was to develop a new formula for the longshore sediment transport rate, to test the formula against a data, and to determine empirical coefficient values, were successfully achieved.

Keywords: Longshore sediment transport, laboratory data, field data, wave energy flux, longshore current, erosion

TABLE OF CONTENTS

LIST OF FIGURES

LIST OF TABLES

LIST OF SYMBOLS

A_c = an empirical coefficient
C = the Chezy coefficient based on d_{50}
g = the acceleration of gravity
s = the relative sediment density (ρ_s/ρ)
ρ_s = the density of the bed material
ρ = the density of water
μ = a ripple factor
τ_{wc} = the bottom shear stress due to waves and current
C_{90} = the Chezy coefficient based on d_{90} (the particle diameter exceeded 10% by weight)
u_o = the maximum wave orbital velocity near the bed
f_w = the wave friction factor
I_1, I_2 = the Einstein integrals
p =the porosity of the sediment
ν = the kinematic viscosity
D_{50} , d_{50} = the dimensionless grain diameter
H_s = the significant wave height
Z = a suspension parameter reflecting the ratio of the downward gravity forces and upward fluid forces acting on a suspended sediment particle in a current
ψ = an overall correction factor representing damping and reduction in particle fall speed due to turbulence
x = a cross-shore coordinate originating at the shoreline and taken positive offshore (b denotes the break point)
z = a vertical coordinate originating at the still-water level
h = water depth
w = the fall velocity (as a function of temperature and grain size)
W_s = the total amount of work
$c(x,z)$ = concentration distribution
F = wave energy flux approaches to the shore
ε = a certain portion, of wave energy flux F used for the work W_s
V = longshore velocity
Q = the total transport rate
U = time-averaged (mean) cross-shore current
V_m = time-averaged (mean) longshore current
F_{bx} = cross-shore component of bottom friction term
F_{by} = longshore component of bottom friction term
L_x = cross-shore component of lateral mixing term
L_y = longshore component of lateral mixing term
R_{bx} = cross-shore component of the wave driving term
R_{by} = longshore component of the wave driving term
S_{xy} = the radiation stress component
S_{yy} = the radiation stress component alongshore
τ_{by} = shear stress component at the bottom

c_f = an empirical bottom friction coefficient
$\in_{i,j}$ = the components of an eddy viscosity tensor, *(i,j = x,y)*
τ = shear stress at the air-water interface
c_D = drag coefficient
ρ_a = density of air
W = wind speed
E = wave energy density
C_g = wave group speed
H = wave height (either at offshore or onshore)
K_1, K_2 = transport coefficient
P_{ls} = wave energy flux factor using the significant wave height in calculation
I = immersed weight longshore transport rate
P_{lr} = energy flux factor using the root-mean square breaker height
H_{brms} = the root-mean square breaker height
ξ_b = Iribarren number
$tan\ \alpha$ = bottom slope in the surf zone
L_o = deep-sea wavelength
H'_{os} = the unfracted deep-water significant wave height
r = the bottom roughness
τ_c = critical bed shear stress
C_1 = coefficient depending on the sediment density, median grain size or fall velocity and the density of sea water
τ_m = maximum shear stress at the bottom
ψ_c = factor different for fine to coarse sand
Φ = dimensionless flow power
f_w = the friction coefficient
S_{hcr}, = the critical Shields parameter
k_b = factor to incorporate bedload
w_e = cross-sectional area of the transport zone
H_c = the characteristic wave height corresponding to a 10% occurrence in the wave height distribution
d_{mean} = mean depth from the shoreline to depth
k_w = a profile factor
T_z = assumed to be equal to the mean wave period
f_{by} = the bottom friction
f = wave friction factor

1 Introduction

1.1 Background

Beaches can change on various time scales from short–duration, dramatic changes to slow almost imperceptible evolution that over time yields significant displacements. Such changes will continue to occur in order to provide a means of dissipating incoming wave energy. This adjustment represents the beach's natural dynamic response to the forces of the sea.

Littoral transport is one of the dynamic features of a beach and the nearshore physical system that is very important for the evolution. *Littoral transport* is defined as the movement of littoral drift in the littoral zone by waves and currents. Two major categories of littoral transport exist: *longshore transport*, the movement that is parallel to the shore, and *on/offshore transport*, the movement that is perpendicular to the shoreline. *Littoral drift* is defined as the sedimentary material that is moving. In beach terminology, an indefinite zone extending seaward from the shoreline to just beyond the breaker zone is called the *littoral zone*. The focus of this report is on longshore transport; therefore there is no attention on discussing the on/offshore transport.

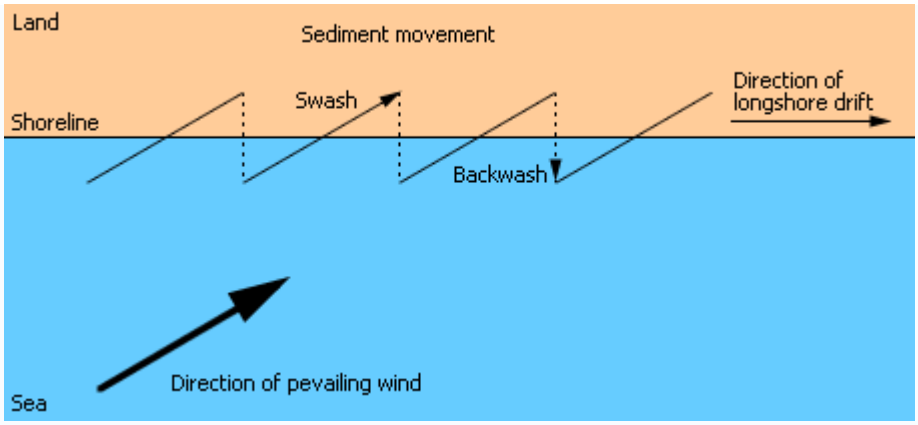

Figure 1 Schematic description of longshore sediment transport.[1]

Schematically described in Figure 1, longshore sediment transport is a process by which sediment moves along the shoreline and it arises when waves approach the beach at an angle (which in turn, are determined by factors such as the prevailing wind and fetch). The incoming waves break at some point, inducing mass transport and turbulence that mobilize sediment and generate a net alongshore movement of water, known as a *longshore current*, which moves the sediment along the shoreline. Waves striking the shore obliquely as opposed to straight on will cause the wave *swash* to move up the beach at an angle. The swash generates a movement of the sediment particles (usually sand or shingle) up the beach at this angle, whereas the *backwash* brings them straight down the foreshore. This has the net effect of a slow movement of the particles along the shore.

[1] http://en.wikipedia.org/wiki/Longshore_drift

Normally the total transport in the surf zone is considerably larger that the transport in the swash zone, but the latter may produce non-negligible contribution. Longshore drift is the principal processes in the build-up of features such as spits[2], bars and tombolos[3].

Figure 1.1 The spit at Spurn Point from the south.[4]

Figure 1.2 The tombolo at Goat Rock Beach in northern California, plan view (left) and side view (right).[5]

As mentioned above, the longshore transport mainly results from the stirring up of sediment by the breaking waves and the movement of this sediment by the longshore current induced in the surf zone by the breaking waves (Shore Protection Manual, 1984). This simple picture of the process will form the basis for the derivation of the transport formula in this report. In general, a direction of the wave approach that produces a large angle of the wave crest to the shoreline promotes longshore transport. The longshore

[2] Spit is a depositional landform found off coast, such as at a cove, bay, ria, or river mouth.
[3] Tombolo is unusual among beach-related landforms, it extends outward from the shore, connecting with an island.
[4] http://www.fortunecity.com/greenfield/ecolodge/25/spurn.htm
[5] http://geology.about.com/library/bl/images/bltombolo.htm

transport magnitude and direction normally varies from season to season, day to day, or even hour to hour, because of the variability in the waves reaching to the shore. The wave approach angle, duration, and wave energy are the major factors that influence the longshore transport rate.

Longshore transport is one of the main causes of coastal erosion. Alongshore gradients in the longshore transport rate results in movement of the shoreline, where a retreat corresponds to erosion and an advance to accumulation. Thus, erosion implies that more sediment is transported away from an area than what is transported to an area. In case of accumulation the opposite prevails. Gradients in longshore sediment transport may arise for natural reasons or because of man-made structures and activities.

During the past three decades, the longshore sediment transport rate has been identified as one of the most important processes to consider in coastal engineering design and analysis. For example, the longshore transport rate is a necessary input required for determining dredging requirements at a port entrance (Schoonees, 2000). In addition, for the design of breakwaters at harbour entrances, navigation channels, beach improvement schemes that incorporate groines, detached breakwaters, and beach fills, and the determination of the stability of inlets and estuaries (Schoonees and Theron, 1993) knowledge on the longshore transport rate is crucial.

Longshore sediment transport rate is, in general, calculated using semi-empirical equations, which are based on laboratory and field data (Shore Protection Manual, 1984; Kumar et al., 2003). Previous studies show that numerous formulas and models for computing the sediment transport by waves and currents have been proposed, ranging from quasi-steady formulas based on the traction or energetics approach to complex numerical models involving higher-order turbulence closure schemes (Larson and Bayram, 2005).

In this report, the evaluation of a newly derived formula was done against six data sets, described in the following, encompassing five field sets and one laboratory data set. Smith *et al*. (2002) conducted longshore transport experiments in a large-scale physical model (LSTF) at the Coastal and Hydraulics Laboratory, during which they measured the longshore sediment transport rates. The longshore transport rates were also computed using the CERC and Kamphuis formulas to evaluate the predictive capability of these formulas. Kraus *et al*., (1989) measured the longshore transport rate across the surf zone using streamer traps (*i.e.*, DUCK85 field experiment). Miller (1998, 1999) measured and calculated rates of sediment transport during five storm events using the Sensor Insertion System (SIS) (*i.e.*, SANDYDUCK field experiments). Schoonees and Theron (1993) created a field data base for longshore sediment transport. They compiled a large number of data sets from a variety sites around the world. Finally, Wang *et al*. (1998) measured the total longshore sediment transport rate in the surf zone using streamer traps at 29 locations along the southeast coast of the United States and the Gulf Coast of Florida. The rate was measured concurrently by traps and by short-term impoundment at Indian Rocks Beach in West-Central Florida (Wang *et al.* 1998).

In order to provide basic knowledge about longshore sediment transport formulas, some well-known sediment transport formulas are briefly discussed, although they are not used to compute the longshore sediment transport rate for the data sets investigated here. The formulas are Bijker's formula, Engelund-Hansen's formula, Watanabe's formula, and some other formulas. Many researchers have dieveloped such sediment transport formulas using different approaches. However, the main focus of this study is to develop a formula of the total longshore sediment transport rate, based on the work by Larson and Bayram (2002).

1.2 Objectives

The main objective of this report is to develop a new formula for the total longshore sediment transport rate. It should be stressed that the new formula is based on the work by Larson and Bayram (2005) as mentioned above. The formula was evaluated with an extensive, high-quality data base including both laboratory and field measurements, which is the second objective of this report. Larson and Bayram calibrated their formula for the sediment transport rate by comparison with the CERC formula. In this report, a more satisfactory evaluation of the formula is carried out through comparison with the compiled data base. Furthermore, typical values on the empirical transport coefficient in the formula is established and related to various physical quantities.

1.3 Procedure

In order to achieve the above-stated objectives, a detailed work plan was developed encompassing theoretical development, data compilation, and formula evaluation as the major steps. First, the new formula for the longshore sediment transport rate was derived. In order to do this, a solid background considering the longshore sediment transport processes was required. A brief review of the knowledge on longshore sediment transport processes is presented in the second chapter of the report. This chapter contains general definitions, modes of transport, and how to estimate longshore sediment transport rates. In addition, some existing sediment transport formulas are reviewed to provide background knowledge on calculating the longshore sediment transport rate. A detailed discussion is presented in chapter three concerning the development of the new formula for longshore sediment transport rate. In order to achieve the second objective in this report, an extensive data set on the longshore sediment transport rates was compiled from the literature encompassing both laboratory and field data. The new formula was evaluated towards the data and empirical coefficient values were determined. The details of the evaluation will be presented in chapter four. Finally, conclusions and some recommendations will be presented in chapter five.

2.0 Longshore Sediment Transport Processes

2.1 Introduction

As mentioned above, littoral drift is the sediment transported in the nearshore zone under the action of waves and currents. The transport rate Q at which the littoral drift is moved parallel to the shoreline is denoted the longshore transport rate. Since this movement is parallel to the shoreline, there are only two possible directions of motion, either to the right or to the left, relative to an observer standing on the shore looking out to sea. Movement toward the left is indicated by the subscript *lL*; movement toward the observer's right is indicated by the subscript *lR*. In practical applications, the direction of the littoral drift is labelled in accordance with compass direction (e.g., north, south, etc.).

Reversal in the transport direction often occurs and waves transport material at different rates depending on their properties, so two components of the longshore transport rate are potentially important. These components are the net rate and the gross rate. In order to clarify the transport direction, transport to the right is denoted as Q_{lR} and taken to be a positive quantity, whereas transport to the left is denoted as Q_{lL} and taken to be a negative quantity. Therefore, the net transport over a certain period (e.g., year) is defined as $Q_{lNET} = Q_{lR} + Q_{lL}$. According to Komar (1998), the *net longshore transport* of sediment is defined as the summation of the movement under all wave trains arriving at the shore from countless wave-generation areas, accounting for the different transport directions. If $Q_{lR} > Q_{lL}$, the net longshore sediment transport rate is directed to the right with a positive value. If $Q_{lR} < |Q_{lL}|$, the net longshore sediment transport rate is directed to the left with a negative value. The net longshore sediment transport rate can range from zero to a large magnitude corresponding to million cubic meters of sand per year.

The gross annual longshore transport is defined as the summation of the temporal magnitudes of the littoral transport irrespective of direction, that is, $Q_{lGROSS} = Q_{lR} + |Q_{lL}|$. There is a possibility to have a very large gross longshore transport at a beach, simultaneously as the net transport is close to zero.

Normally, the net longshore transport may be related to the deposition versus erosion of beaches on opposite sides of breakwaters or jetties, whereas the gross longshore transport is used to predict shoaling rates in navigation channels and natural inlets. The gross longshore transport has been identified to be the major factor in determining jetty length, and the frequency and cost of maintenance dredging, and whether or not the inlet can function at any cost.

However, most shorelines consistently have a net annual longshore transport in one direction. Determining the direction and average net and gross annual amount of longshore transport is important in developing shore protection plans. The rate depends on the local shore conditions and shore alignment, as well as the energy and direction of the incident wave.

2.2 Modes of Sediment Transport

Once in motion, the transport path (or mode of transport) that sediment grain takes is largely determined by the mass of the grain and the velocity of the current and or waves. Sediment transport is traditionally categorized into two modes, that is, bed load and suspended load (Figure 2).

2.2.1 Bed load

Grains transported as bed load are supported by either continuous contact (traction) or intermittent contact (saltation) with the bed. In the case of traction, the grains slide or roll along, maintaining contact with the bed at all times. This is relatively slow form of transport and is typical when weak currents are transporting sands or strong currents are transporting pebbles and boulders. In the case of saltation, the grains take short hops along the bed. Saltation is typical when moderate currents are transporting sand or strong currents are transporting gravel and pebbles.

2.2.2 Suspended load

Grains transported as suspended load are supported by the turbulence in the fluid. The grains may make intermittent contact with the bed, but on average they spend most of their time in suspension. The grain paths of suspended load are distinguishable from saltation due to their irregularity, which arises from the grains being buffeted by turbulent eddies in the current. Suspension transport is typical when moderate currents are transporting silts or strong currents are transporting sands. Grains transported as wash load are permanently in suspension, and typically consist of clays and dissolved material.

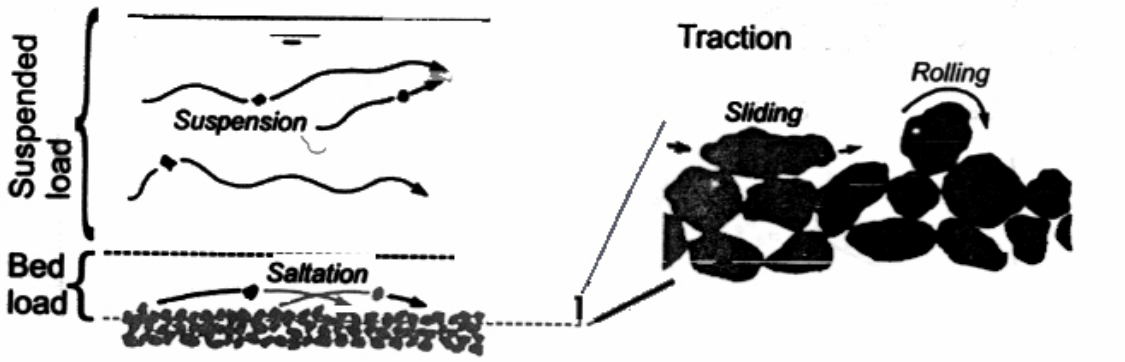

Figure 2 Schematic representations of sediment transport modes showing grain paths. Note that bed load includes both saltation (jump) and traction. (Masselink and Hughes, 2003).

It is difficult to separately measure these two modes of transport and to determine which one is dominant under a specific set of conditions. Because suspended load transport is more readily measured than bedload transport, it has been the subject of a considerable

number of studies. These studies demonstrate that suspension concentration decrease with elevation above the bottom. In the breaker zone suspended load is normally considered to be larger than bed load with peaks in the concentration (and transport rate) around the point of incipient breaking and at the base of the swash zone (Komar, 1998). Lower concentrations have typically been found at mid-surf positions. When a portion of the wave energy reflected back to sea, there is a correlation between individual suspension events and the incident breaking wave period. Long-period water motions may account for significant sediment suspension, especially close to the shoreline (Coastal Engineering Manual, 2002).

2.3 Estimating Longshore Sediment Transport Rates

2.3.1 Field Measurements

Longshore sediment transport rates can be measured in the field using different techniques that have been developed during the last five decades, such as sediment tracers, short-term impoundment, streamer sediment traps, and various instruments (optical backscatter sensors, pumping samplers, etc.).

Tracer theory and operational aspects of this method were reviewed by Galvin (1987), Madsen (1987, 1989), and Drapeau *et al.* (1991) (see Wang *et al.*, 1998). Patterns of beach sediment movement can be obtained by introducing some kind of tracer, such as sand tracers, shingle tracers, silt tracers, dye tracers, and bacteria tracers. These are deposited on a beach or in the nearshore zone at a particular point or along a selected profile, and surveys are made subsequently to see where the tracers have gone. In order to reproduce the movements of the natural beach sediment, a tracer must consist of particles similar in size, shape and with similar hardness and the same specific gravity as the sediment already present. It must also be possible to identify the tracer after it has moved along the beach or across the sea floor. Some part or the entire amount of tracer may become buried within a beach, and a proportion may be lost seaward from the nearshore zone.

Sand that is naturally or artificially coloured can be used as tracer, but there are difficulties in observing coloured grains when they form only a small proportion of the sediment on a beach. More effectively is the use of natural or artificial sand coated with a colloidal substance containing a fluorescent dye (Bird, 1996). Sand labelled in this way is injected into the surf zone, and the beach material is sampled on a grid to determine the subsequent tracer movement. By counting the numbers of tracer grains in each grid sample, the local concentrations are determined, and these values serve to establish the contours of tracer concentrations (Komar, 1998). Those concentrations in turn permit a measure of the mean longshore transport distance of tracer movement during the period of transport. Hence, the mean longshore advection velocity of the sand on the beach is obtained. Usually the time between injection of the tracer and the sampling is an hour to a few hours. So, the measurement of the longshore sand transport is assumed to be under relatively fixed wave conditions. Tracer techniques could provide measurements that are suitable for correlations with waves and longshore currents at a short time scale but not

particularly useful to determine long-term net transport rates or directions. There are indications that transport rates derived from tracers consistently over-estimate the actual rate (Van Wellen *et al.*, 2000). This is because of the temporal and spatial variability of both the depth disturbance and width of the active beach, which are important parameters when calculating transport rates from tracer measurements. The variability of these parameters during a tide, for example, has not yet been taken into account (Van Wellen *et al.*, 2000). In spite of this there are numerous studies that used sand tracers to determine sand transport rates, including Komar and Inman (1970), Inman *et al.* (1980), and Kraus *et al.* (1982). The sediment tracer method is an indirect technique. Sediment fluxes are derived by separately quantifying the vertical and horizontal movement of the tracer (Wang *et al.*, 1999).

Figure 2.1 From the left, an example of sand tracer, viewed under a low magnification microscope, a shingle tracer in use in a littoral environment, and a dye-and-drogue tracking study.[6]

Instruments such as optical backscatter sensors (OBS) have been developed with capability to measure sediment concentration within the water column in great detail at time scales corresponding to fractions of a second (Miller 1999). The wave breaking region tends to be associated with high concentrations of sediment within the water column. Yu *et al.* (1993) did some measurements using OBS, and the results showed that maximum values in the sediment concentration occur in the vicinity of incipient wave breaking. The data from all transects studied showed the same trend, with highest concentrations occurring in regions of wave breaking and bore formation. Sternberg *et al.* (1984) used five arrays of OBS sensors with simultaneous current measurements at Leadbetter Beach, Santa Barbara, California and found a single peak in the longshore sediment flux distribution near the mid-surf location between the bar and the beach. Similar peaks near the midsurf position were found in the data used for this study (SANDYDUCK: 11 November 1995 and 12 March 1996). Sternberg et al. found the flux to always decrease shoreward and seaward which differs from the analysis of data in this study, which found peaks near the swash zone for several storms (SANDYDUCK: 12 March, 27 March, and 2 April 1996). Although optical techniques are capable of providing measurements with high spatial and temporal resolution, they have not been broadly used for many reasons. High cost, lack of reliable field calibration, and omission of the bed load remain the major obstacles (Wang *et al.*, 1999).

[6] http://www.environmentaltracing.info

Traps are one of the techniques for determining sediment transport rate, especially for the suspension load. The traps consist of a vertical array with sample bins that collect sediment, but at the same time they allow water to pass through. Therefore, the vertical distribution of suspended sediment and associated transport rate can be determined. Traps can be placed at any location across the surf zone (Inman *et al.* 1980; Kraus, Gingerich, and Rosati 1988). Numerous studies indicate that the main portion of longshore sediment transport takes place in the surf and swash zones. The only method at present that has been identified for bed load transport measurement is traps (Coastal Engineering Manual, 2002). Bedload traps consist of a number of bins, which are open-ended, or dug into the seabed, the place where most of the bedload transport takes place. There are questions about the sampling efficiency when traps are used in the nearshore because of the potential for scour (Rosati and Kraus, 1989).

The impoundment method (blocking of the longshore transport rate by a structure) has been used to estimate the longshore sediment transport rate. Longshore sediment transport estimates using this method is believed to provide results that are closest to the total quantities (i.e., the bed load plus suspended load transport), and typically represents long-term measurements (i.e., weeks to years). These long-term, total transport quantities are central to practical coastal engineering design. In short-term impoundment applications, the structure is constructed temporarily (only for the purpose of the longshore sediment transport rate measurement) prior to the experiment and will be removed after completing the experiment. Bodge (1986) described an example of longshore sediment transport rate measurement using this method (Wang *et al*., 1999). Those measurements were conducted by constructing a specially designed sandbag groin in order to intercept the longshore sediment transport. The volume transport rate was computed by quantifying the morphological change updrift and downdrift of the groin.

2.3.2 Laboratory Experiments

When faced with a problem which is complicated and that defy rigorous mathematical treatment from first-principles, an attractive option is to solve the problem through laboratory experiments. Thus, laboratory experiments are common in sediment transport investigations and many have been conducted. Using large-scale sediment transport facilities (for example, the LSTF; see Figure 2.2) to conduct experimental work yields reliable measurements of longshore sediment transport rates. However, in small-scale facilities, employing the resulting data set to establish empirical formulas valid for field scale conditions has been questioned, since simultaneous fulfilment of geometric (sediment diameter), Froude (waves), and Reynolds (turbulence) similarity is impossible to achieve. Kamphuis (2002) (see Smith *et al.*, 2002) argued that carefully executed experiments, although conducted at a relatively small scale, could be performed with limited scale effects. In the laboratory environment, uncertainties are less than that of field results (Smith *et al.*, 2002). It may be difficult to improve longshore sediment transport rate estimates based on field data only because of uncertainties associated with measuring basic variables and the subjectivity in interpreting the results (Smith *et al.*, 2002). Improvements to sediment transport relationships are more easily developed from controlled and controllable model test, despite the shortcomings of physical models.

However the ultimate test of any developed transport relationship is comparisons with field data.

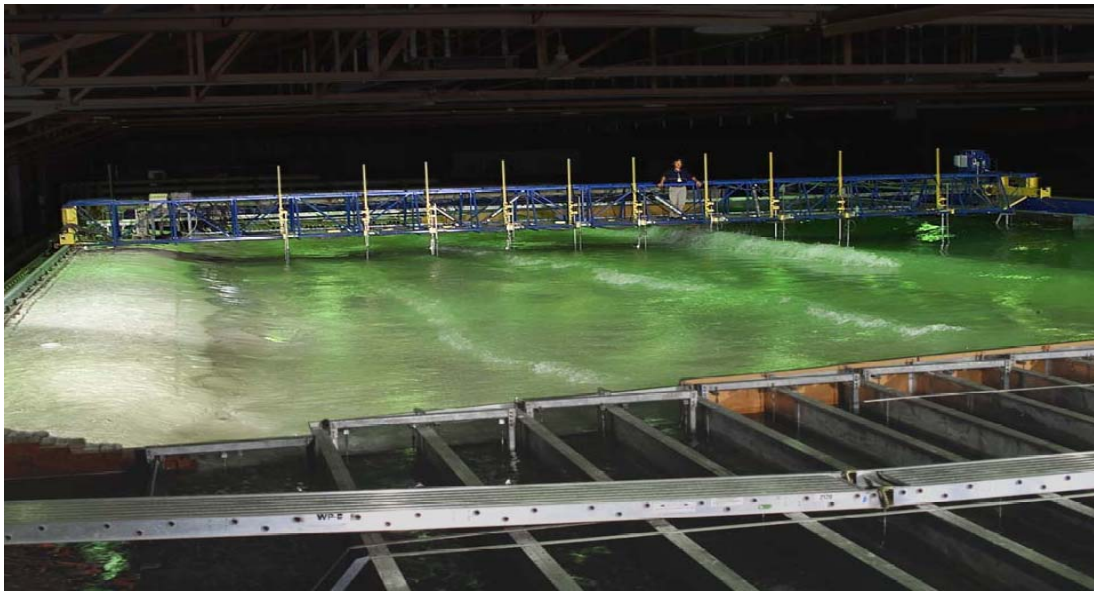

Figure 2.2 An experiment on longshore sediment transport conducted in the LSTF.[7]

2.4 The Existing Longshore Sediment Transport Equations

A number of different longshore sediment transport formulas have been proposed through the years. In Schoonees (2001), several of these formulas were reviewed and classified according to the following approaches:

(a) Energetics or energy flux approach;
(b) Shear stress or modified steady flow approach;
(c) An approach using the product of the shear stress and the longshore current velocity;
(d) Dimensional analysis;
(e) Combining the predictions of the suspended concentration and the longshore current velocity;
(f) Empirical methods.

In this chapter, some of the most important existing longshore sediment transport formulas will be discussed (not in too great detail) with respect to the approach taken. Chapter 3 will focus on the new formula developed based on the work by Larson and Bayram (2005).

[7] http://web.engr.oregonstate.edu/~scottc2/pdf/Smith_2003.pdf

2.4.1 The Energy Flux Approach

The most well-known and applied formula for the total longshore sediment transport is the so-called CERC formula presented in the Shore Protection Manual formula (SPM)**,** which is published by the US Army, Corps of Engineers (1984). The general formula is written as,

$$Q_{SPM} = K_1 P_{ls} \qquad [m^3/year]$$

where:

K_1	= 1289 for prototype conditions	[m^4/W.year]
P_{ls}	= wave energy flux factor using the significant wave height in calculation	[W/m].

An alternative formulation of the SPM formula is,

$$I = K_s P_{ls} \quad \text{or} \quad I = K_r P_{lr}$$

where:

I	= immersed weight longshore transport rate;
P_{lr}	= energy flux factor using the root-mean square breaker height;
K_s	= 0.5 (0.78)
	= 0.39 if the significant breaker height is used; and
K_r	= 0.78 if the root-mean square breaker height (H_{brms}) is used.

Many researchers contributed to the development of the SPM formula, including Watts (1953), Caldwell (1956), Inman and Bagnold (1963), Komar (1969), Komar and Inman (1970) and Komar (1983) (see Schoonees and Theron 1994).

Swart (1976) (see Schoonees 2001) developed a transport coefficient K_1 that is a function of median grain size (D_{50}) to produce a modified version of the SPM formula,

$$Q_{SWART} = K_2 P_{ls} \qquad [m^3/year]$$

where:

K_2	= 1876 $\log_{10}$	[D_{50} in unit meter,m]
	= (0.00146/D_{50}).	

In general, the coefficient K_1 needs to be investigated in order to see whether its value is influenced by any parameters or not. Kamphuis and Readshaw (1978) and Vitale (1981) studied the coefficient, K_1 and found that K_1 is a function of the surf similarity parameter, also known as Iribarren number, ξ_b.

This Iribarren number may be written as,

$$\xi_b = \frac{\tan\alpha}{\left(H_{brms}/L_o\right)^{0.5}}$$

where:

tan α	= bottom slope in the surf zone;
H_{brms}	= $H_{bs}/\sqrt{2}$; and
L_o	= deep-sea wavelength.

Unlike Kamphuis and Readshaw (1978), Vitale (1981) (see Schoonees 2001), decided to use the mean wave height measured in deep water instead of H_{brms}. However, in order to avoid the need to calculate the wave height at the breaker line, the relationship proposed by Kamphuis and Readshaw (1978) and Readshaw (1979) was adapted,

K_p'	= 0.7 ξ_b	for $0.4 < \xi_b < 1.4$
	= 1.24	for $\xi_b \geq 1.4$

with,

Q_s	= $K_p' P_{ls} / 2g$	[kg/s]; and

$$Q_{Vitale} = \frac{31557600 Q_s}{(1-p)\rho_s} \qquad [m^3/year].$$

where:

p	= porosity of the sediment (assumed to be 0.4 for sand);
ρ_s	= density of the sediment (2650 kg/m^3 for sand).

2.4.2 The Shear Stress (Modified Steady Flow) Approach

The methods that have been categorized in this group vary from simple to complicated formulations. Thus, it is not possible to give one general equation in order to summarize the different formulas. Basically, these formulas are derived from formulas for sediment transport in rivers, which have been adapted for application to coastal conditions.

Based on the Kalinske–Brown bedload formula, which was an early formula developed for rivers, Iwagaki and Sawaragi (1962) (see Schoonees 2001), proposed a new formula for the total longshore sediment transport rate using the shear stress approach. The formula is expressed as:

$$Q_{IS} = \frac{8583.10^8 H_{bs}^{2/3}\left(\tan\alpha\right)^{4/3} T_z^{1/6} \cos\theta_b P_{ls}^{1.5}}{g^{5/3}\left(\rho_s - \rho\right)^{1.5} D_{50}^{0.5}\left(\sin 2\theta_b\right)^{1/6} L_b^{1.5}} \qquad [m^3/s \text{ per m}]$$

Iwagaki and Sawaragi assumed that H_{bs} is equal to H'_{os},

where:

H'_{os}	= the unrefracted deep-water significant wave height;
D_{50}	= the mean grain size;
$\tan \alpha$	= bottom slope in the surf zone;
T_z	= assumed to be equal to the mean wave period;
θ_b	= wave angle at breaker line;
p	= porosity of the sediment (assumed to be 0.4 for sand);
ρ_s	= density of the sediment (2650 kg/m^3 for sand).
L_b	= wavelength at breaker line; and
P_{ls}	= wave energy flux factor using the significant wave height in calculation.

Frijlink (1952) (see Schoonees 2001) proposed a bedload formula that was adapted by Bijker (1967). Bijker modified the formula by introducing the average bed shear stress, which was caused by a combination of waves and current, instead of current only. Bijker expressed the local bedload rate Q_{bi} as,

$$Q_{bi} = \frac{5D_{50}vg^{0.5}}{C_h}\exp\left(\frac{-0.27(\rho_s - \rho)D_{50}C_h^2}{\rho\mu v^2\left(1 + 0.5(\xi_{BK}u_o / v)^2\right)}\right)$$

where:

v	= longshore current velocity;
μ	= ripple coefficient
	= $(C_h/C_{D90})^{1.5}$;
C_{D90}	= 18 $\log_{10}$ $(12d/D_{90})$;
u_0	= maximum orbital velocity at the bed according to linear theory;
ξ_{BK}	= coefficient with two values, namely, ξ_1 and ξ_2;
ξ_1	= 0.0575 C_h; and
ξ_2	= $C_h (f_w/2g))^{0.5}$.

Two values of the bottom roughness r have been used to obtain C_{h1} and C_{h2}, where for C_{h1}, $r = 2.5\ D_{50}$ (according to Nielsen, 1979) and for C_{h2}, it can be calculated by using the method introduced by Swart (1976b):

$$C_h = 18\log_{10}(12d / r)$$

Bijker utilized the Einstein approach to obtained the local suspended load rate, Q_{si},

$$Q_{si} = 1.83Q_{bi}\left[I_1 In(33d / r) + I_2\right]$$

where:

I_1, I_2	= the Einstein integrals.

Finally, the total local longshore transport rate, Q_{ti} proposed by Bijker (1967) is,

$$Q_{ti} = (Q_{bi} + Q_{si})f \qquad [m^3/s \text{ per m}]$$

or:

$$Q_{ti} = 31557600\, f(Q_{bi} + Q_{si}) \qquad [m^3/\text{year per m}]$$

Engelund and Hansen (1967) (see Schoonees 2001) proposed a formula, which was similar to Bijker's formula. Subsequently, Swart (1976b) modified this formula. Thus, the total local longshore sediment transport rate formula derived by Engelund, Hansen and Swar**t** is written,

$$Q_{ti(E,H,S)} = \frac{0.05vC_h(\tau_{wc}/\rho)^2 \rho f}{g^{2.5} D_{50}(\rho_s - \rho)} \qquad [m^3/s \text{ per m}]$$

where:

τ_{wc} = bed shear stress due to waves and current combined;
f = wave friction factor.

As in Bijker's formula, ξ_2 and C_h are determined using the bottom roughness r from the Swart (1976b) method. The quantity C_h is recomputed at each depth and not only at the breaker line.

2.4.3 The Product of the Shear Stress and the Longshore Current Velocity Approach

A general transport formula can be expressed as,

$$Q = C_1 v^{m_2} (\tau - \tau_c)^{m_2}$$

where:

τ = bed shear stress;
τ_c = critical bed shear stress;
m_2 = exponent either 1.0 or 1.1; and
C_1 = coefficient depending on the sediment density, median grain size or fall velocity and the density of sea water.

Most of the formulas that belong to this category contain an incipient motion criterion *(τ_c).*

Watanabe (1985) and Watanabe *et al.* (1988, 1991) (see Schoonees 2001) investigated sediment transport due to waves and a mean current combined. If the mean current corresponds to the longshore current velocity, the formula will predict the longshore

transport rate (Schoonees, 2001). Thus, the Watanabe formula for the total longshore transport rate per unit width can be expressed as,

$$q_c = A_c v(\tau_m - \tau_c)/(\rho g)$$

where,

Q_i = 31 557 600 f q_c [m^3/year per m];
A_c = 0.5 for model applications;
= 2.0 for prototype cases;
τ_m = maximum shear stress at the bottom; and
τ_c = critical shear stress;

with:

τ_c = 0 in the surf zone;
= $(\rho_s - \rho)g\, D_{50}\, \psi_c \tanh^2 (K_c\, (x - x_b)/x_b)$ outside the surf zone;
K_c = 1.0;
ψ_c = factor different for fine to coarse sand; and
D_{50} = median grain size.

By integrating the local rate across the surf zone and beyond, the total longshore transport rate can be determined.

Katori *et al.* (1984) (see Schoonees 2001) conducted an experiment in a cross-flow tank. Kraus *et al.* (1988) employed the sediment transport measurements collected by Katori *et al.* and data taken from the SUPERDUCK experiment to develop a predictive formula. The Kraus *et al.* formula for the total load per unit width can be expressed as,

$$Q_i = 31557600 \Phi w D_{50} f \qquad [\text{m}^3/\text{year per m}]$$

where:

f = wave friction factor;
Φ = "dimensionless flow power"

= 0.85 $S_h^{1.1}$;

S_h = $\dfrac{(\tau_m - \tau_c)v}{\rho[(\rho_s - \rho)gD_{50}/\rho]^{1.5}}$; and

τ_m = 0.5 $f_w \rho (u_o^2 + v^2)$.

The horizontal bottom orbital velocity u_o was computed based on linear theory. Using the explicit formula proposed by Swart (1974) (see Schoonees 2001), the friction coefficient f_w could be calculated. It was assumed that the bottom roughness is 2.5 D_{50} (Engelund and Hansen, 1967; Nielsen, 1979) (see Schoonees 2001). The total transport rate is obtained by integrating across the surf zone and beyond.

2.4.4 Dimensional Analysis Approach

Based on dimensional analysis, Kamphuis *et al.* (1986) (see Schoonees 2001) proposed a formula for the total transport rate according to,

$$Q = 1.28 \tan \alpha_k H_{bs}^{3.5} \sin 2\theta_b / D_{50}$$

where:

Q	= total longshore transport rate	[kg/s]; and
$\tan \alpha_k$	= beach slope defined as d_b/x_b.	

Using the same approach (dimensional analysis), Sánchez-Arcilla *et al.* (1988) (see Schoonees 2001) derived the following bulk formula,

$$I_l = 0.5(\rho_s - \rho) A_s \xi^{0.5222} 10^{-0.1908\xi} H_{bs}^{2.5} \sin 2\theta_b g^{1.5} .(S_h^c - S_{hcr}^c)$$

and,

$$Q_{Sanchez} = \frac{31557600 I_l f}{(\rho - \rho) g (1 - \rho)} \quad [\text{m}^3/\text{year per m}]$$

where:

A_s	= coefficient
	= 4.88E-03;
S_h	= a version of the Shields parameter
	= $\rho H_{bs} / (\rho D_{50})$; and
c	= 0.4419.

In addition, in the expression for Q above, 0.5 is included as a factor. The critical Shields parameter, S_{hcr}, is 12.77, and the significant wave height should be used in the formula.

2.4.5 The Suspended Sediment Concentration and the Longshore Current Velocity Approach

Tsuchiya (1982) (see Schoonees 2001) derived a total longshore transport rate formula,

$$Q_r = C_1 (\rho / \rho_s) I_T d_b^{2.5} g^{0.5} \sin 2\theta_b \quad [\text{m}^3/\text{s}]$$

where:

C_1	= 5 $\pi c_2 \alpha_T$ / (16 f_w);
c_2	= 0.2;
f_w	= 0.3; and
α_T	= $L_b H_{bs} / (2 T_p g d_b^{1.5})$.

He also mentioned that for prototype conditions, value of I_T should be taken as 0.3. Thus, the final bulk longshore transport formula of Tsuchiya is given by:

$$Q_{TSUCHIYA} = 31557600\, fQ_T$$

Tsuchiya (1982) (see Schoonees 2001) used the significant wave height and the peak wave periods as representative wave quantities.

Voitsekhovich (1986) (see Schoonees 2001) proposed another version of a bulk longshore transport formula. The formula was derived in terms of the mean concentration and mean longshore current velocity in the surf zone yielding a transport,

$$Q = k_b v_{mean} C_{mean} w_e \qquad \text{[kg/s]}$$

where:

k_b = factor to incorporate bedload
= 1.2;
v_{mean} = mean longshore current velocity in the surf zone;
C_{mean} = mean concentration in the surf zone; and
w_e = cross-sectional area of the transport zone which extends up to a depth d_v (d_v is typically 1 to 1.5 d_b).

Therefore,

$$Q_{VOITSEKHOVICH} = \frac{31557600Qf}{(1-p)\rho_s}$$

In order to determine the parameters v_{mean}, C_{mean}, and w_e, Voitsekhovich developed predictive equations for each of them,

$$v_{mean} = \frac{33.3H_c^2 \sin 2\theta_b}{T_s^2 (g d_{mean})^{0.5}}$$

where:

H_c = the characteristic wave height corresponding to a 10% occurrence in the wave height distribution;
= 1.072 H_{bs} (using a Rayleigh distribution);
d_{mean} = mean depth from the shoreline to depth d_v;
= 0.5 d_v [for planar beach condition];
d_v = 0.09 γL_b;

For,

$$C_{mean} = \frac{0.5 \times 10^{-4} \varepsilon H_c^2 (1 + \sin 2\theta_b)}{d_{mean} T_z (g D_{50})^{0.5}}$$

where,

ε = 1.65E03 [kg/m^3];

and,

$$w_e = \frac{0.4 \times 10^{-2} g d_b T_z^2}{k_w \tan \alpha \gamma^2}$$ [for planar beach];

where,

k_w = a profile factor;
= $d_v / (2\, d_{mean})$;
= 1 [for planar beach];

and:

T_z = assumed to be equal to the mean wave period.

3 A New Formula for Longshore Sediment Transport

3.1 General

In Chapter 2, six well-known formulas for computing the longshore transport rate were reviewed based on different approaches. Although these formulas were previously evaluated with data, predictions by the formulas may differ since the amount and quality of the data sets employed for evaluation varied significantly. In order to provide reliable and robust predictions of longshore transport rate an extensive data set is needed that covers a wide range of wave, sediment, and beach conditions. Also, most of the existing formulas, only consider wave-generated currents (which is the case for the CERC formula), and disregard other mechanisms, such as wind and tidal currents that could influence the longshore sediment transport.

Due to these limitations, an effort was made in this study to provide an alternative formula for computing the longshore sediment transport rate. This formula should be possible to apply to the case of sediment transport by wind and tidal currents, not only wave-generated currents, and the formula should be validated with an extensive data set including a wide range of conditions.

Larson et al. (2005) proposed a new formula for the longshore sediment transport rate. They assumed that suspended sediment the dominant mode of transport in the surf zone, since the bottom sediment is stirred up (suspended) by the strong wave action. Generally, in the nearshore zone, it is believed that breaking waves suspend most of the transported sediment, and less sediment is suspended outside the surf zone implying less transport in this region. Thus, the presence of breaking waves is needed to mobilize sediment, whereas any type of current (e.g., wave-generated, wind, tidal) can transport the sediment. In the next section, a brief summary of the derivation of the formula is presented.

3.2 Development of a New Longshore Sediment Transport Rate Formula

Waves approaching the coastline obliquely generate longshore currents. These longshore currents transport the sediment that has been stirred up by breaking waves in the surf zone. Here, it is assumed that wave breaking stir up sediment and maintain an average concentration distribution *c(x,z)*, where *c* is in units of m^3 sediment/m^3 water. The total amount of work (W_s); which is needed to keep the sediment in suspension at steady-state is,

$$W_s = \int_0^{x_b} \int_0^{h(x)} c(x, z)(\rho_s - \rho) g w dz dx$$

where:

x	= a cross-shore coordinate originating at the shoreline and taken positive offshore (b denotes the break point);
z	= a vertical coordinate originating at the still-water level and pointing downwards;
h	= water depth; and
w	= the fall velocity (as a function of temperature and grain size).

The wave energy flux that approaches to the shore is F and a certain portion, ε of this wave energy flux is used for the work W_s, therefore, $W_s = \varepsilon F$. This assumption yields:

$$\varepsilon F = (\rho_s - \rho) g w \int_0^{x_b} \int_0^{h(x)} c(x, z) dz dx$$

If the longshore sediment transport rate is the product between the local concentration and longshore velocity (V), the total transport rate may be written as:

$$Q = \int_0^{x_b} \int_0^{h(x)} c(x, z) V(x, z) dz dx$$

Assuming a constant longshore current yields:

$$Q = V \int_0^{x_b} \int_0^{h(x)} c(x, z) dz dx$$

Replacing the integral using the relationship above that includes the fraction of the incoming wave energy used for keeping the sediment in suspension gives:

$$Q = \frac{\varepsilon}{(\rho_s - \rho)(1 - a) g w} FV \qquad \text{(eq 3.1)}$$

It the above equation, the porosity (a) was added in the denominator. The value of the transport coefficient (ε), which expresses the efficiency of the waves in keeping sand grains suspended, is unknown. One possibility to determine the value of ε is through comparison against field or laboratory data (which is done in this study). Another option is to calibrate towards the CERC formula, assuming that is widely applied and well-tested formula yields reliable estimates. In order to carry out such comparisons, expressions for the longshore current *(V)* and the wave energy flux *(F)* are needed. In the next section (3.2.1), a derivation of an appropriate expression for the longshore current is presented, whereas in the section 3.2.2, the wave energy flux will be discussed.

An advantage of using the new formula is for the case when wind- or tide-generated currents need to be included in the transport formula. A first approach would be to simply add mean currents in the surf zone from waves, wind, and tide linearly.

3.2.1 Longshore current

By applying a simple alongshore momentum equation, linearized friction, and ignoring lateral mixing, an expression for the longshore current can be written as,

$$\frac{2}{\pi}\rho c_f u_o V = \frac{dS_{xy}}{dx} \qquad \text{(eq 3.2)}$$

where:

c_f	= a friction coefficient;
u_0	= the bottom orbital velocity; and
S_{xy}	= the radiation stress directed alongshore and transported onshore.

Assuming shallow water condition, the following relationships hold:

(a) Linear wave theory gives a representative value of the maximum near-bottom wave orbital velocity:

$$u_o = \frac{1}{2}\sqrt{\frac{g}{h}}H = \frac{1}{2}\gamma\sqrt{gh}$$

(b) Within the surf zone, the ratio of wave height, H to water depth is taken as:

$$H = \gamma h$$

(c) The radiation stress directed alongshore and transported onshore according to Longuet-Higgins, 1970 (see Masselink, G., & Hughes, M.G. 2003) is:

$$S_{xy} = \frac{1}{16}\rho g \gamma^2 h^2 \sin 2\alpha$$

(d) The Snell's law for refraction (small angles):

$$\frac{\alpha_b}{\sqrt{hg_b}} = \frac{\alpha}{\sqrt{hg}}$$

Then, substituting the above expressions into the governing equation (eq 3.2), and employing a Dean-type equilibrium beach profile ($h=Ax^{2/3}$), the longshore current can be expressed as:

$$V = \frac{5}{48}\frac{\pi\gamma\sqrt{g}}{c_f} A^2 \frac{x^{1/3}}{\sqrt{h_b}} \sin 2\alpha_b$$

However, in the above formula the current varies across the profile, so we need to determine a representative current to use in the longshore sediment transport rate formula (eq 3.1). For that purpose the average current is determined from,

$$V_m = \frac{1}{x_b}\int_0^{x_b} V dx = \frac{5}{64}\frac{\pi\gamma\sqrt{g}}{c_f} A^{3/2} \sin 2\alpha_b \qquad \text{(eq 3.3)}$$

in which,

$$A = \frac{9}{4}\left(\frac{w^2}{g}\right)^{1/3}$$

is the relationship between A and fall velocity (w) taken from Kriebel *et al.*(1991).

Derivation of equation 3.2

A brief background to the derivation of eq 3.2 is outlined in the following. The vertically integrated, time-averaged momentum equation may be written (Mei 1983) (see Kraus and Larson, 1991),

$$U\frac{\partial U}{\partial x} + V\frac{\partial U}{\partial y} = -g\frac{\partial \eta}{\partial x} + F_{bx} + L_x + R_{bx} + R_{sx} \qquad \text{(eq 3.4)}$$

$$U\frac{\partial V}{\partial x} + V\frac{\partial V}{\partial y} = -g\frac{\partial \eta}{\partial y} + F_{by} + L_y + R_{by} + R_{sy} \qquad \text{(eq 3.5)}$$

where:

U	= time-averaged(mean)cross-shore current	[m/s];
V	= time-averaged(mean)longshore current	[m/s];
F_{bx}	= cross-shore component of bottom friction term	[m/s^2];
F_{by}	= longshore component of bottom friction term	[m/s^2];
L_x	= cross-shore component of lateral mixing term	[m/s^2];
L_y	= longshore component of lateral mixing term	[m/s^2];
R_{bx}	= cross-shore component of the wave driving term	[m/s^2];
R_{by}	= longshore component of the wave driving term	[m/s^2];

R_{sx} = cross-shore component of the wind (surface) driving term [m/s^2];

R_{sy} = longshore component of the wind (surface) driving term [m/s^2].

Since we only consider the longshore component, taken to be in the y-direction, only eq 3.5 will be used for the derivation of equation 3.2.

Wave-driving terms

The wave-driving term is a function of the change in radiation stresses that takes place as waves propagate towards shore and transform by shoaling, refraction, and breaking. It is expressed as,

$$R_{by} = -\frac{1}{\rho d}\left(\frac{\partial S_{xy}}{\partial x} + \frac{\partial S_{yy}}{\partial y}\right) \qquad \text{(eq 3.6)}$$

where the radiation stress component directed and transported alongshore (S_{yy}) is:

$$S_{yy} = \frac{1}{8}\rho g H^2\left[n\left(\sin^2\theta + 1\right) - \frac{1}{2}\right]$$

Bottom friction terms

Bottom friction is expressed as a quadratic stress law in the total local fluid velocity and is produced by the combination of steady motion from the mean wave-, wind-, and tidal-induced current and unsteady motion from oscillatory waves. The instantaneous shear stress components at the bottom is written,

$$\tau_{by} = c_f \rho\sqrt{u^2 + v^2}\,v$$

where c_f is an empirical bottom friction coefficient, and v the y-component of the total current velocity (evaluated at the bottom).

Noting that F_{by} is not identical to the shear stress but is by definition the shear stress component divided by water density and total depth:

$$F_{by} = -\frac{c_f}{d}\left\langle\sqrt{u^2 + v^2}\,v\right\rangle \qquad \text{(eq 3.7)}$$

In this equation, triangular bracket denotes a time-averaging operation over the interval of a wave period.

Lateral mixing terms

The lateral mixing terms describe the horizontal exchange of momentum and are related to the turbulent Reynolds stresses. Lateral mixing, which is not well understood in the nearshore, is typically modeled using an eddy viscosity approach.

The mixing terms may be expresses a general form as,

$$L_y = \frac{1}{d}\left[\frac{\partial}{\partial x}\left(\in_{yx} d\,\frac{\partial V}{\partial x}\right) + \frac{\partial}{\partial y}\left(\in_{yy} d\,\frac{\partial V}{\partial y}\right)\right] \qquad \text{(eq 3.8)}$$

where:

$\in_{i,j}$ *(i,j = x,y)* are the components of an eddy viscosity tensor.

Wind-driving terms

Birkemeier and Dalrymple (1975) (see Kraus and Larson 1991) developed a numerical model that considered the local wind in nearshore circulation. Local wind often constitutes an important forcing in the nearshore. When wind blows over a water surface, it promotes a current, and the surface will tilt in adjustment of the water body to the transfer of momentum at the air-sea interface. Wind-generated currents have been detected at depths on the order of 100m, and strong winds can produce significant setup and setdown at the shoreline during storms. The wind stress appears as a forcing term in the momentum equations and can be expressed using a quadratic drag law,

$$\tau_s = c_D \rho_a w^2$$

where

c_D	= drag coefficient;	
ρ_a	= density of air	[kg/m^3]; and
W	= wind speed	[m/s].

In the general case of a wind blowing at a nonzero angle to the shoreline, the driving terms describing the wind can be written as

$$R_{sy} = \frac{c_D \rho_a}{\rho d} |W| W \sin\varphi \qquad \text{(eq 3.9)}$$

The alongshore force balance (eq 3.2) can be obtained based on the following assumptions:

a. Linear-wave theory is applicable everywhere, both inside and outside the surf zone.
b. The time-averaged cross-shore current U is zero.
c. The bottom contours are straight and parallel, indicating uniformity in the y-direction ($\delta/\delta y=0$).
d. Bottom friction in the cross-shore direction is small in comparison with $\delta S_{xx}/\delta x$. (Retaining the cross-shore friction term couples the momentum equations)

These assumptions imply that all convective acceleration terms in eq 3.5 is zero. The remaining terms in the y-longshore component momentum (eq 3.5) are wave driving (eq 3.6), bottom friction (eq 3.7), lateral mixing (eq 3.8) and wind driving (eq 3.9). Eq 3.5 may thus written,

$$\frac{d}{dx}\left(\in d\,\frac{dV}{dx}\right) - f_{by} = \frac{1}{\rho}\frac{dS_{xy}}{dx} - c_D\,\frac{\rho_a}{\rho}|W|W\sin\varphi \qquad \text{(eq 3.10)}$$

where f_{by} is defined as:

$$f_{by} = -F_{by}d$$

Using the linear approximation to evaluate the bottom friction yields:

$$f_{by} = \frac{2}{\pi}c_f u_m V$$

Then, substituting this into eq 3.10, neglecting lateral mixing and wind driving, the alongshore force balance becomes as in eq 3.2 above.

3.2.2 Wave Energy Flux

The energy flux F of a wave can be defined as the average energy per unit time and per crest width transmitted in the wave propagation direction. It can also be written as the product of the force acting on a vertical plane located normal to the direction of wave propagation times the particle flow velocity across this vertical plane (Sorensen, 1994). Thus, the energy flux normally incident to the shoreline can be expressed as,

$$F = \frac{1}{T}\int_0^T\int_{-d}^0 (p + \rho g z)u\,dz\,dt$$

where *p* is the dynamic pressure. By introducing the dynamic pressure and the horizontal particle velocity from linear wave theory and integrating, the above equation yields,

$$F = \frac{\rho g H^2 L}{16T}\left(1 + \frac{2kd}{\sinh 2kd}\right)$$

which can be written:

$$F = \frac{E}{T}\left[\frac{1}{2}\left(1 + \frac{2kd}{\sinh 2kd}\right)\right] \qquad \text{(eq 3.11)}$$

With the following definition,

$$n = \frac{1}{2}\left(1 + \frac{2kd}{\sinh 2kd}\right)$$

equation 3.11 becomes:

$$F = \frac{nE}{T} = nEC \qquad \text{(eq 3.12)}$$

The term *n* is a function of *kd*, or the relative depth *d/L*, and for deep water the value on *n* is 0.5, whereas for shallow water it is 1.0. For the present case, we will assume that the water condition corresponds to shallow water.

For a wave that is not normally incident, the wave energy flux is given by,

$$F = EC_g \cos \alpha \qquad \text{(eq 3.13)}$$

where

E	= wave energy density	[Nm/m^2]; and
C_g	= wave group speed	[m/s].

and the angle was introduce through $\cos \alpha$.

The wave energy density is written using linear-wave theory as,

$$E = \frac{1}{8}\rho g H^2$$

where

ρ	= density of water	[kg/m^3];
g	= acceleration produced by gravity	[m/s^2]; and
H	= wave height (either at offshore or onshore).	[m]

The group celerity C_g is related to the phase celerity of the individual waves in the group (C) through the factor n:

$$C_g = nC$$

For deep-water conditions, the group celerity is,

$$C_{go} = \frac{gT}{4\pi}$$

whereas for shallow-water conditions, it is:

$$C_{gb} = \sqrt{g\frac{H}{\gamma}}$$

4 Evaluation of New Longshore Transport Formula

4.1 Review of Longshore Transport Database

In this study, five high-quality data bases on the longshore sediment transport rate were employed of which one included laboratory data and four field data. In the selection of these data bases, accuracy and reliability in the measurements were primary criteria for inclusion in the evaluation. The compilation of the data bases consists of wave and sediment characteristics at a variety of locations, and the longshore transport rate. The predictive capability of the newly derived formula for the longshore transport rate (described in Chapter III) was evaluated using the databases. Only brief background descriptions concerning the experiments are provided in the following section, whereas data reviews are included in Appendix A.

4.1.1 Laboratory Data Database

Large-Scale Sediment Transport Facility (LSTF) data

Experiments were conducted by Smith et al. (2002) in the LSTF at the Coastal and Hydraulics Laboratory of the US Army Engineer Research and Development Center in Vicksburg, Mississippi. The LSTF is a large-scale laboratory facility, which is 30 m wide, 50 m long, and 1.4 m deep, and it is designed with a capability of simulating conditions comparable to low-energy coasts (Figure 2.2). The main objectives of the investigation was to simulate surf zone processes found on a long, straight, natural beach in a finite-length basin, and to upgrade the existing methods of computing the total longshore sediment transport rate. A beach was constructed having a trapezoidal shape and consisting of 150 m^3 of fine quartz sand with $d_{50} = 0.15$ mm. The sand cover was 0.25 m thick, and it extended 27 m alongshore and 18 m offshore. In order to minimize variation in transport due to alongshore differences in waves and current characteristics, the beach was constructed with shore-parallel bottom contours.

Since the boundaries of the finite-length beach were identified to cause some disturbances, the wave-driven currents were supplemented by an external recirculation system. The recirculation system has 20 independent vertical turbine pumps located in the cross-shore direction at the downdrift boundary. Flow channels located upstream of each pump were used to direct flow to the pump. Each pump has a variable speed motor to control the discharge rate. The LSTF also contains a 21 m long bridge across the beach with the purpose of instrument mounting and experimental observation. Single-wire capacitance-type wave gauges were used to measure the water surface elevation. Thus, wave heights were measured by placing ten gauges on the bridge. Also, a gauge was located in front of each wave generator in order to collect the offshore wave characteristics.

The total velocities were measured using ten acoustic Doppler velocimeters (ADVs), which were placed at the same cross-shore positions on the bridge as the wave gauges

(separated by 40 cm). Twenty 0.75 m wide traps situated at the downdrift boundary were used to estimate sediment flux. Longshore sediment transport rates were obtained using eighteen traps that were installed in the flow channels and two additional traps placed landward of the first flow channel. Each trap was equipped with three load cells, which was capable to weigh the amount of trapped sand.

4.1.2 Field Data Database

DUCK 85 surf zone sand transport experiment

In September 1985, the Duck85 surf zone sand transport experiment was performed at the U.S. Army Corps of Engineers Field Research Facility (FRF) at Duck, North Carolina. In these experiments, Kraus et al. (1989) used streamer traps to measure the cross-shore distribution of the longshore sediment transport rate. They conducted eight experimental runs, and during a certain time, the amount of sediment transported at a specific location in the surf zone was collected with the traps placed opposed to the direction of the longshore current. The photopole method was employed to measure wave height and wave period. This method involved filming the water surface elevation at poles placed at approximately 6m intervals across the surf zone utilizing as many as 16mm synchronized cameras (Larson and Bayram, 2002). Each day the bottom profile was surveyed along the photopole line, and measured profiles had shelf-type shapes during the entire experiment. Overall, the DUCK85 experiment (see Table A.2 in Appendix A) included the root-mean-square wave heights (H_{rms}) at the most offshore pole in the range of 0.4-0.5m, and peak spectral period (T_p), in the range between 9 and 12 sec. During the experiments, long crested waves of cnoidal form arrived from the southern quadrant, producing a longshore current moving to the north with a measured magnitude of 0.1-0.3 m/sec.

SANDYDUCK (1 and 2) surf zone sand transport experiment

There are two different data bases from the SANDYDUCK experiment, denoted as SANDYDUCK 1 and SANDYDUCK 2 (just for the purposes of this report and to avoid any confusion). SANDYDUCK was also conducted at FRF, but the experiment was conducted during several major storms (Miller, 1998, 1999). The Sensor Insertion System (SIS), which is a diver-less instrument deployment and retrieval system that can operate in seas with individual wave heights up to 5.6 m, was used for sediment transport measurements (Miller, 1999). The standard SIS consists of Optical Backscatter Sensors (OBS) to measure sediment concentration, an electromagnetic current meter for longshore and cross-shore velocities, and a pressure gauge for wave and water levels. The measurement results concerning wave conditions and mean longshore current velocities (for SANDYDUCK 1 and SANDYDUCK 2) are described in Table A.3 and A.4 (Appendix A). The data sets were taken along the research pier, which is a 561 m long concrete and steel structure equipped by widely spaced (12 m apart) and 1-m diameter steel pilings.

Schoonees and Theron Field Data Compilation

The field data compiled and reviewed by Schoonees and Theron (1993) contains 123 cases with measured longshore transport rates, including data on other parameters such as wave and sediment characteristics. The data were collected on beaches from a variety of sites all around the world. Transport data encompass particulate (non-cohensive) sediment (including sand, gravel, and shingle) transported alongshore from the swash zone across the surf zone to deep water (Schoonees and Theron, 1993). Originally, the measurements involved both total rates and local transport rates. In Table A.5 (see Appendix A) all the details are presented concerning the total rates.

Wang et al. surf zone sediment transport experiment

Wang *et al.* (1998) performed field experiments along the southeast coast of the United States and the Gulf Coast of Florida between September 1993 and May 1995. They measured the total rate of longshore sediment transport in the surf zone, mostly by using streamer traps. Twenty-nine streamer trap experiments and one short-impoundment experiment were performed under low-energy conditions. The selected sites represented a wide range of morphodynamic and hydrodynamic conditions. Seven out of twenty-nine of the trap experiments were performed on barred coast with waves breaking on the longshore bar (Wang *et al.,* 1998). Eighteen trap experiments were placed on coasts with negligible offshore bar influence on the wave breaking. The remaining experiments were placed in the inner surf on barred coasts because of operational difficulties due to high waves and a deep bottom trough. Twelve field sites among the twenty-nine field sites had a plunge step at the breaker line or the secondary breaker line for the case of the barred coasts. In Table A.6 (see Appendix A), hydrodynamic and morphodynamic conditions, as well as the measured total rate of longshore sediment transport, are reviewed.

Based on 20 measured wave heights from video image, the root-mean-square (*rms*) wave height was calculated and ranged from 0.1 to 0.8 m (low wave-energy conditions). The trap measurements were made under of plunging, spilling, and collapsing wave conditions. The measurements of the incident wave angle were in the range of 2 to 35 deg. In the Florida Panhandle, waves generated by local wind prevailed. The wave period ranged from less than 3 sec to more than 10 sec. Sediment properties varied from one site to another, with the average bottom sediment grain size ranging from 0.17 mm to 2.25 mm.

4.2 Evaluating the Formula and Discussion

Measured hydrodynamic and morphodynamic properties in each experiments were employed in the longshore sediment transport formula. Since computation of the longshore transport rate is dependent on the incident wave height and angle at breaking, direct measurements of such quantities is highly useful. If input parameters from an experimental case contain measured breaking wave parameters the longshore transport

rate could be obtained without additional calculations. However, not all the six data sets provided input data to the same detail. For example, two data sets (*i.e.*, SANDYDUCK 2 and Wang *et al.*,) provided the root-mean-square wave height, H_{rms}, whereas the other four data sets (*i.e.*, LSTF, Duck85, SANDYDUCK 1, and Schoonees data) measured the significant wave height. In addition, if the input parameters did not provide breaking wave conditions, the needed parameters were obtained by employing the equation for conservation of wave energy flux and Snell's law from the measurement point to the break point (for example, for the SANDYDUCK data).

In Appendix B, all calculations of longshore sediment transport rate using the six data sets are presented. Each data set may include slightly different computations since the input data vary. However, the main equations (eq 3.1 for the longshore sediment transport rate, eq 3.3 for the average longshore current, and eq 3.13 for the wave energy flux) were used in all calculations.

For the laboratory data set, the breaking wave parameters were measured (see Table A.1 in Appendix A), which makes the transport computations easier. In DUCK85, the needed parameters (breaking wave parameters) were also measured including the average longshore current. In SANDYDUCK 1, the input data were collected at deep-water conditions, so an extra calculation needed to be done in order to obtain the breaking wave parameters (see details in Appendix B), whereas for SANDYDUCK 2, all important parameters were measured. The main difference in the analysis of these three data sets (DUCK85, SANDYDUCK 1 and SANDYDUCK 2) was that the angle of incidence at breaking was assumed small in the breaking wave calculations. For the Schoonees and Theron data set and Wang et al. data sets, the computations were generally the same as for the other data sets.

Another assumption that was employed in all breaking wave calculations, except for the laboratory data set, was the value of the breaker depth index γ. The classical value of γ=0.78 was used to determine breaking wave conditions in shallow water. When estimating the wave energy flux, it is not necessary to use the wave conditions at breaking. Instead the wave energy flux can be estimated at any water depth, for example deep water, if energy losses are neglected as the waves travel from the depth of interest to the break point (e.g., see calculations for SANDYDUCK 2 in Appendix B).

After computing the total longshore sediment transport rate, graphs were developed showing the predictions versus the measured longshore sediment transport rate. The predicted transport rates are plotted without including the empirical transport coefficient (ε), implying that the quantity on the horizontal axis represents some kind of transport parameter. Thus, the slope of the line corresponds to ε.. Graphs were constructed for each data set and the results can be seen in Figures 4 to 4.5. Overall, the agreement displayed in the graphs is good, with the points clustering around a straight line, although significant scatter occurs for some data sets.

Figure 4 shows the result for the LSTF data. Three points are very close to the line, whereas one point is a little bit further away from the line. The result probably indicates

that the breaker type is a factor in estimating longshore transport rate. Overall, spilling breakers show less transport than plunging breakers for otherwise equivalent wave conditions. In Figure 4.1, which displays the DUCK85 data, the points are significantly more scattered around the line, but the reason for this deviation is not known. Kraus *et al.* (1989) conducted their experiment in the feeder current of a rip current, and the transporting current was not directly generated by the incident breaking waves. However, since the velocity in the feeder current was measured, the transport formula should still be able to provide a reasonable quantification of the transport. The current was measured at two locations only in the surf zone, so the estimation of the mean current velocity might not be accurate enough.

Looking at Figure 4.2, which shows the data points for SANDYDUCK 1, one point is significantly below the line, whereas the other four points are located above the line. This distribution around the line produced marked scatter and less good predictions. One reason for the scatter might be the uncertainty introduced through the computations of the longshore current. The measurements were collected during storm condition, which contribute to the high total sediment transport rate (almost 0.5 m^3/s; compare with the DUCK85 measurement taken during low-energy wave conditions). The data points for SANDYDUCK 2 (Figure 4.3) display less scatter around the line compared to SANDYDUCK 1, which implies better predictions. During this experiment, the longshore current velocity was measured and this improved the accuracy of the predictions, since the longshore current velocity is one of the main parameters when calculating the longshore sediment transport rate (equation 3.1).

The graph of measured versus predicted longshore sediment transport rate shown in Figure 4.4 is based on the data set provided by Schooness and Theron (1993). Again there seems to be a fair amount of scatter, but the points are clearly clustered around the line, supporting the applicability of the new formula. The data set is obtained from sites all over the world, providing a very important compilation for evaluating the new formula. Some points are located quite far away from the line and they tend to be clustered in the groups. This is probably because the data were taken from a wide range of sites, as well as measurement methods, which may introduce some bias in the data set. For example, the method employed when measuring the longshore sediment transport rate, and the conditions at the site where the experiments were conducted varied greatly.

The graph in Figure 4.5, illustrating the agreement for the Wang *et al.* (1998) data set, shows less scatter and the points are better clustered around the line. The experimental cases in this data set were carried out under controlled conditions during a limited period of time, yielding increased accuracy compared to the data compiled by Schooness and Theron (1993). During the experiments, the hydrodynamic and morphologic conditions were carefully recorded at each of the field sites. In addition, the measurements of longshore sediment transport rate were collected using two accurate methods, streamer traps and short-term impoundment. Also, the measurements were carried out for low-energy waves, making it easier to achieve higher accuracy. All these factors make it more likely to achieve good agreement with the newly developed formula.

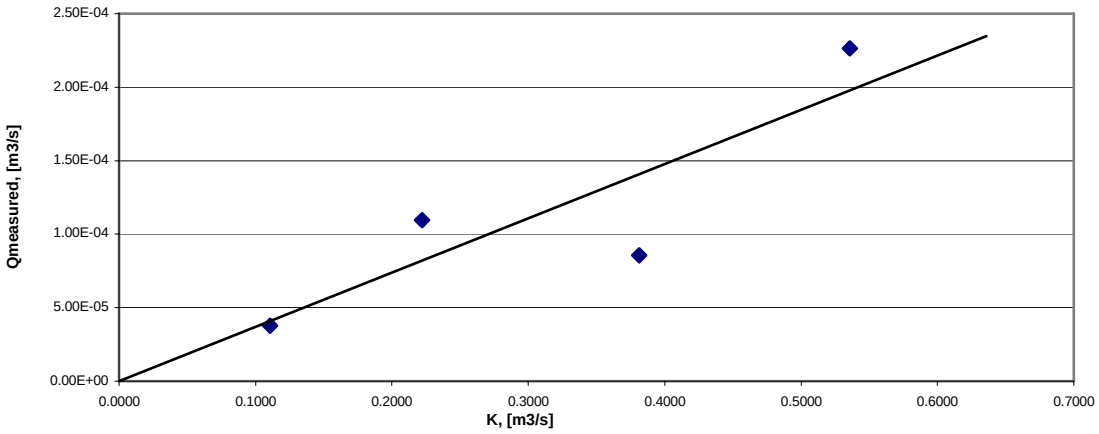

Figure 4 Measured versus predicted total longshore sediment transport rates for the laboratory data - LSTF

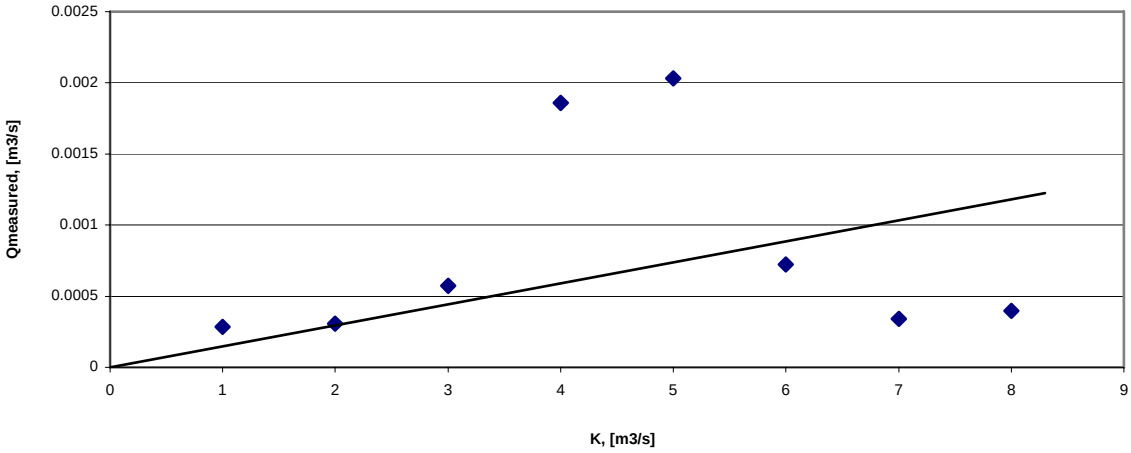

Figure 4.1 Measured versus predicted total longshore sediment transport rates for field data – DUCK85

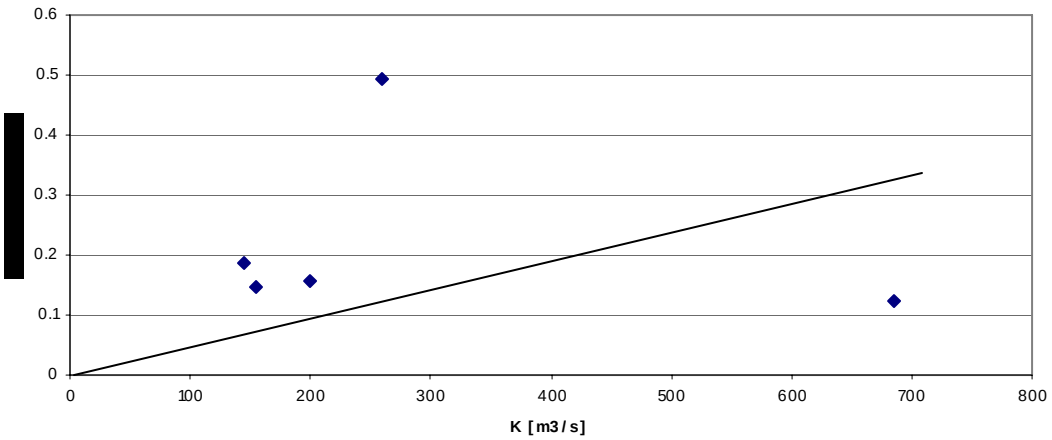

Figure 4.2 Measured versus predicted total longshore sediment transport rates for field data – SANDYDUCK 1

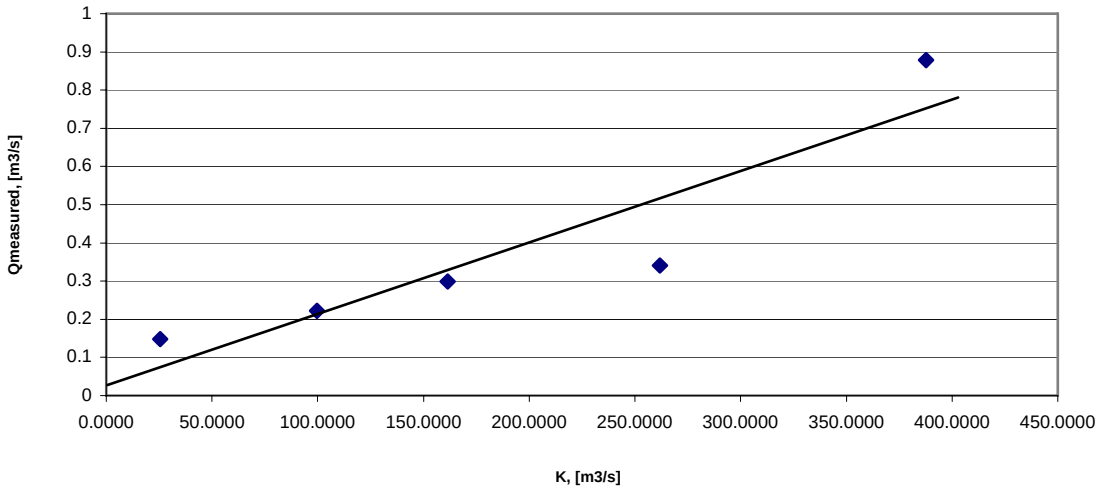

Figure 4.3 Measured versus predicted total longshore sediment transport rates for field data – SANDYDUCK 2

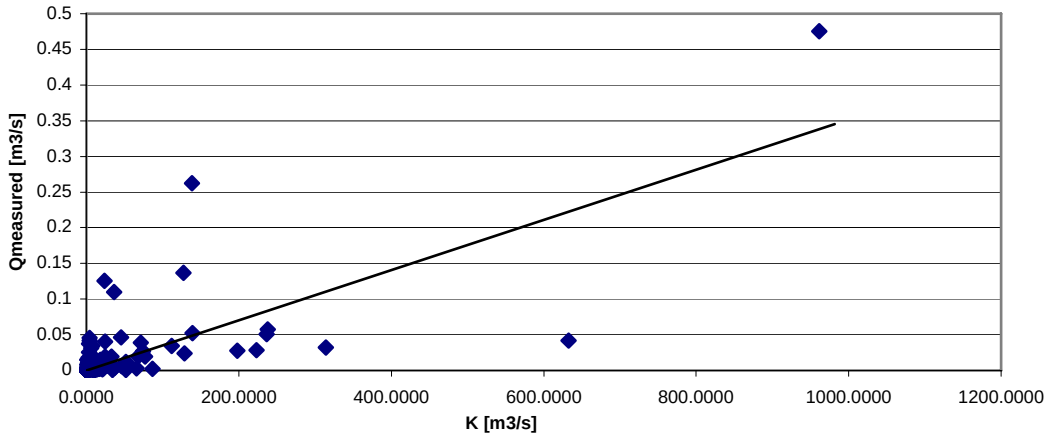

Figure 4.4 Measured versus predicted total longshore sediment transport rates for field data – data base compiled by Schoonees and Theron, 1993

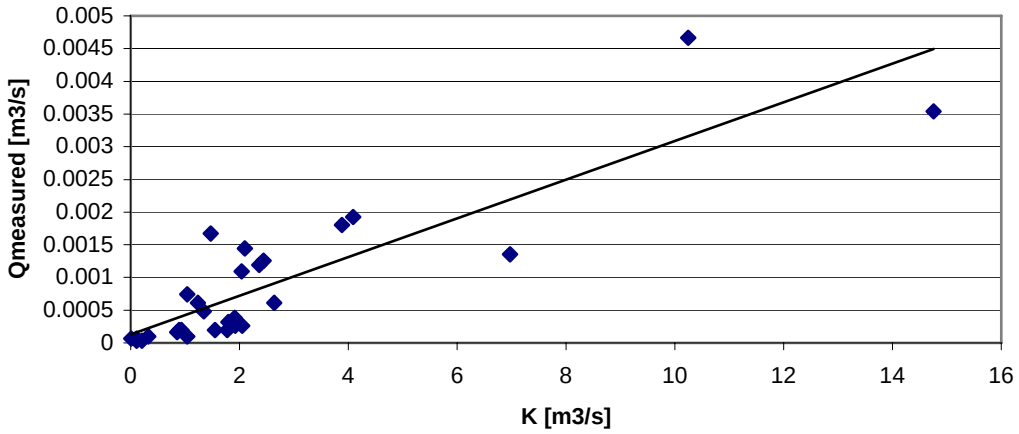

Figure 4.5 Measured versus predicted total longshore sediment transport rates for field data by Wang *et al.*,1998

Figure 4.6 shows a combination of all data sets, plotted with a logarithmic scale to better allow for comparison. The points display a significant scatter and there seems to be a clustering of the points with regard to the specific data set.

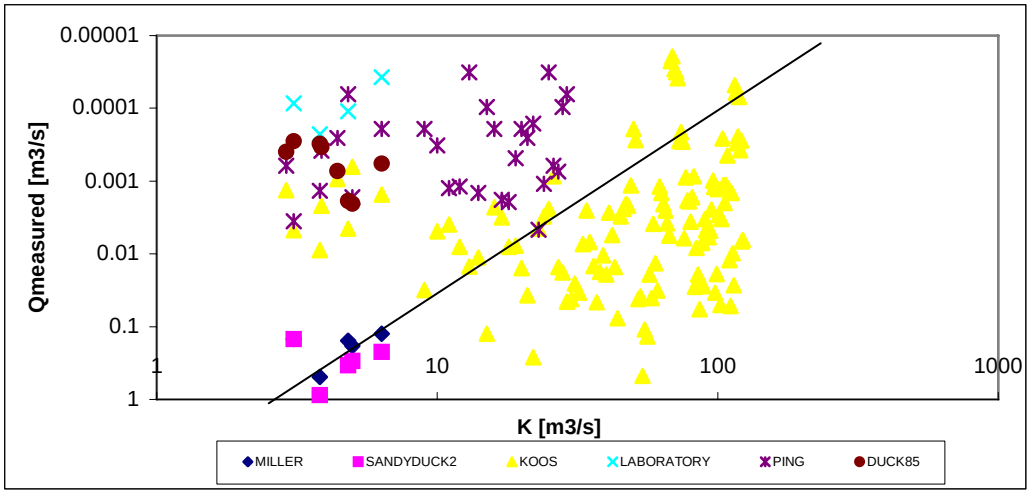

Figure 4.6 Measured versus predicted total longshore sediment transport rates (combination of all data sets)

Investigation of the transport rate coefficient, ε

Each data set yielded fairly good agreement with the new formula, producing results that were more or less evenly distributed around a straight line. However, when all the data sets were plotted together large scatter was observed. This could in part be explained by the fact that the transport rate coefficient ε has a dependency on some physical parameter not resolved by the simple theoretical model. Thus, it was decided to investigate if ε could be correlated with some wave and sediment properties.

The value of ε was estimated for all experimental cases in each of the investigated data bases. The mean of this coefficient was in the range of 0.00018 to 0.0052 for the different data sets, whereas the standard deviation varied from 0.0001 to 0.0024. In Figure 4.7 to 4.11, the relationship between ε and wave period, root-mean-square wave height, significant wave height at breaking, fall velocity, and grain size, respectively, is shown. From Figure 4.7, it is obvious that no direct relationship could be found between ε and wave period. Similarly, no relationship was observed between ε and wave height, if the root-mean-square wave height outside the surf zone was employed (Figure 4.8). However, a clear relationship is found if the significant wave height at breaking is used in the calculations, as it can be seen in Figure 4.9. Similar agreement can be found between ε and grain size, and between ε and fall velocity. Thus, the analysis (based on Figure 4.7 to 4.11) indicates that among the factors that control ε, significant wave height at breaking, grain size, and fall velocity are the most significant.

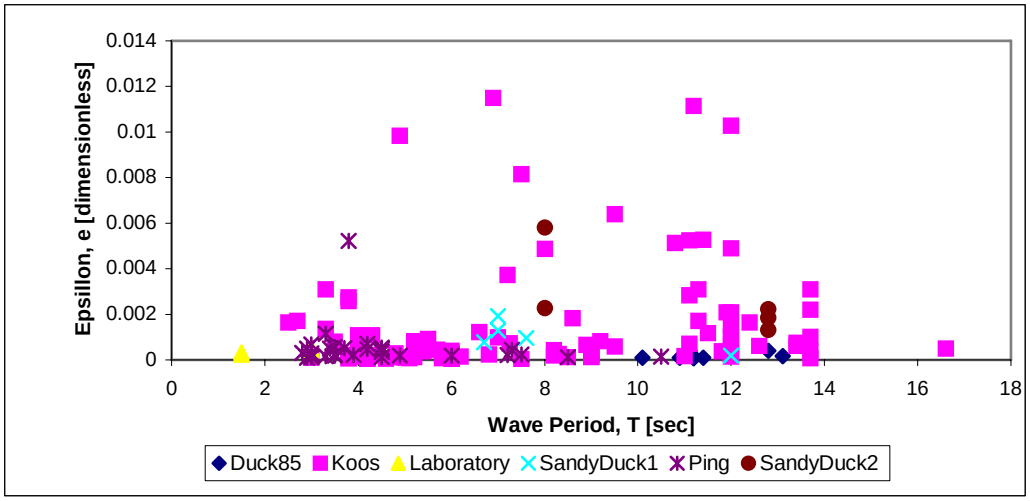

Figure 4.7 The transport rate coefficient ε versus wave period.

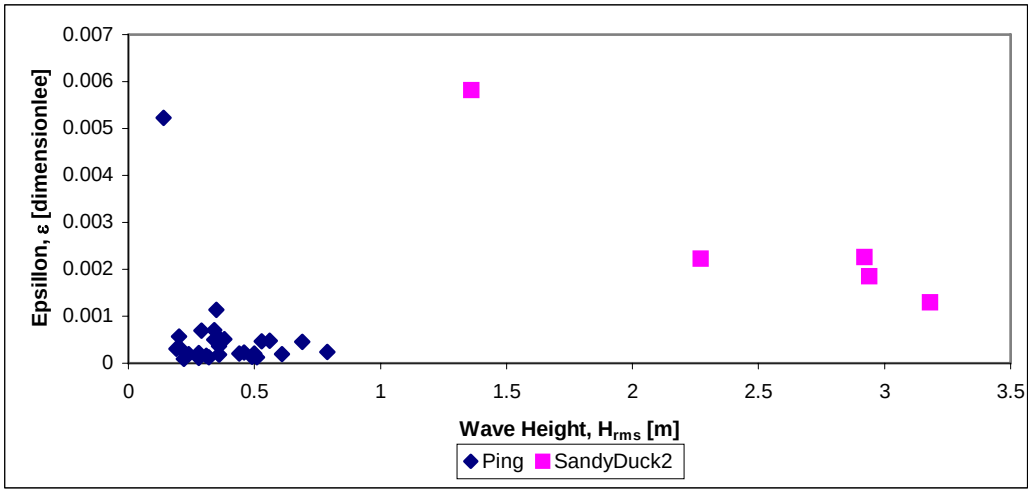

Figure 4.8 The transport rate coefficient ε versus root-mean-square wave height.

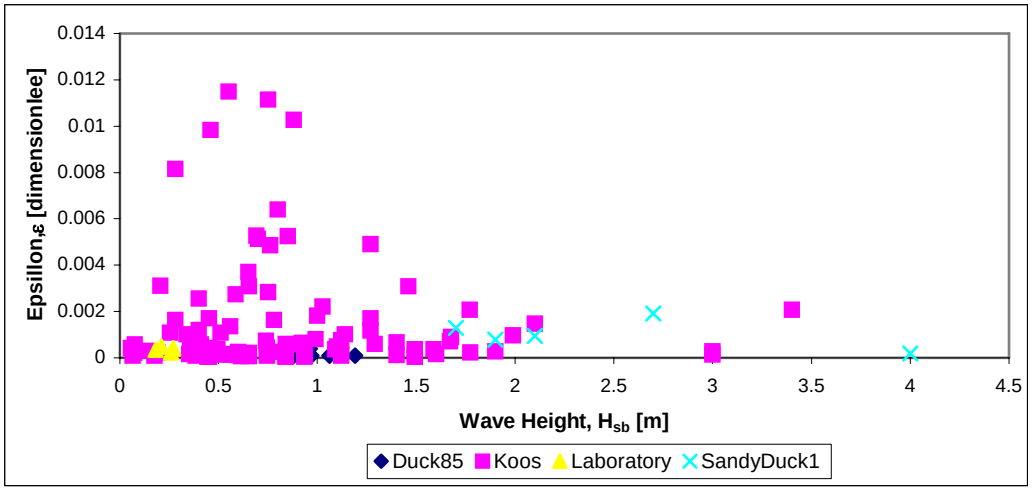

Figure 4.9 The transport rate coefficient ε versus significant wave height at breaking.

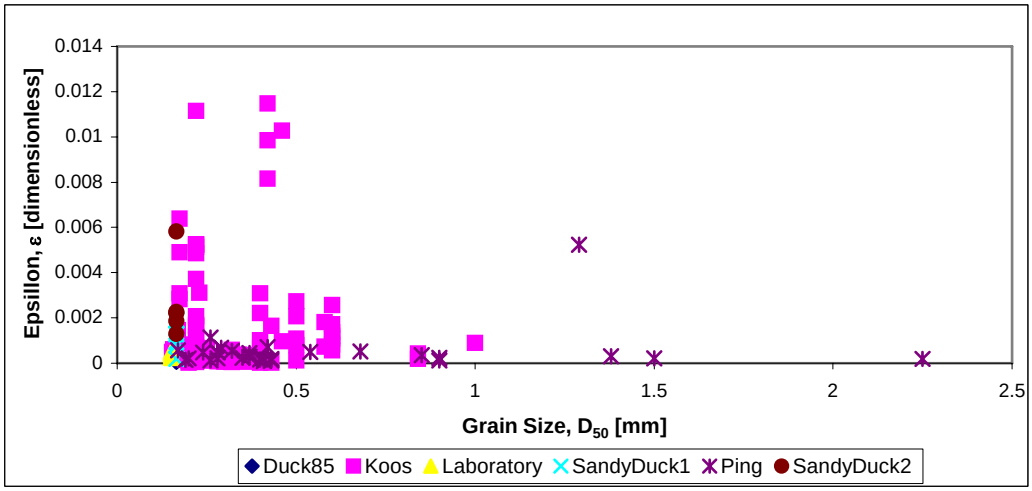

Figure 4.10 The transport rate coefficient ε versus grain size.

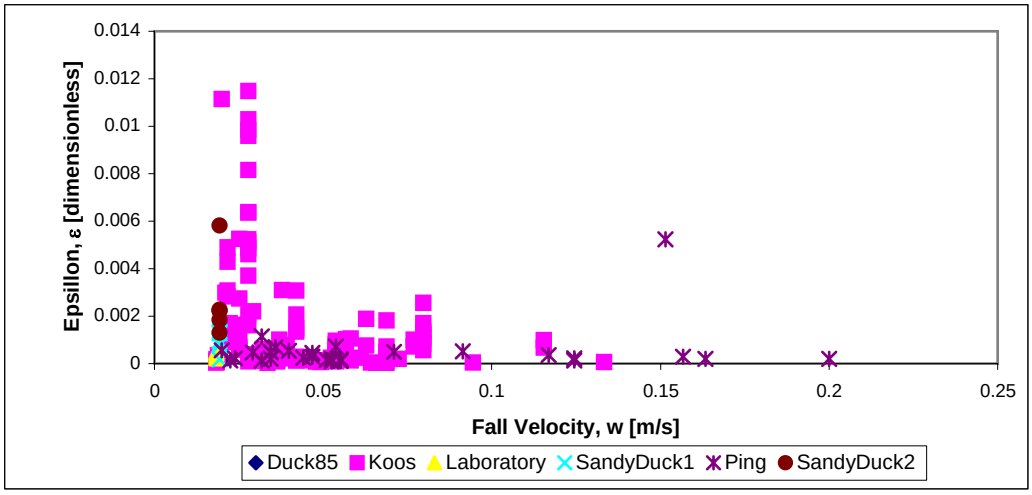

Figure 4.11 The transport rate coefficient ε versus fall velocity.

5 Conclusions

In general, based on comparisons with a number of high-quality data sets on the total longshore transport rate, the newly developed formula yielded overall good predictions. The patterns observed in the graphs showing the agreement between measurements and predictions are similar for all data sets with fairly even clustering around a straight line. However, occasionally there are a few points that scatter far away from the main group of points. This may not only be due to predictive failure of the formula, but it could be argued that the accuracy of the measurements or additional calculations could contribute to the deviations.

In this report, one of the objectives was to find appropriate values on the empirical transport coefficient ε. Results of the analysis show that calculated coefficient values were in range between 0.00018 and 0.0052 for the studied data sets, whereas the calculated standard deviations ranged from 0.0001 to 0.0024. Plots of ε versus selected wave and sediment properties were made in order to examine if additional factors, not included in the theoretical model, could influence ε. The results indicate that fall velocity; significant wave height at breaking, and grain size could be among the factors that control ε.

In conclusion, the objectives in this report to develop a new formula for the total longshore sediment transport rate, to evaluate the formula against data, and to determine values on the empirical coefficient were successfully achieved.

6 References

Bijker, E.W. (1968), "Littoral Drift As Function Of Waves And Current," Proceedings 11th International Conference On Coastal Engineering, ASCE, 415-435.

Bird, E.C.F. (1996), "Beach Management," John Wiley & Sons Ltd, Baffins Lane, Chichester, West Sussex, England.

Bodge, K.R. (1989), "A Literature Review Of The Distribution Of Longshore Sediment Transport Across The Surf Zone," Journal of Coastal Research, 5(2), 307-328.

Greer, M.N., and Madsen, O.S. (1978), "Longshore Sediment Transport Data: A Review," Proceedings 16th International Conference On Coastal Engineering, ASCE, 1563-1576.

Inman, D.L., Zampol, J.A., White, T.E., Hanes, D.M., Waldorf, B.W., and Kastens, K.A. (1980), "Field Measurements Of Sand Motion In The Surf Zone," Procedings 17th International Conference On Coastal Engineering, ASCE, 1215-1234.

Kamphuis, J.W. (1991), "Alongshore Sediment Transport Rate," Journal of Waterway, Port, Coastal, and Ocean Engineering, 117(6), 624-641.

Kamphuis, J.W., (2002), "Alongshore Transport Rate of Sand," Proceedings 28th International Conference on Coastal Engineering, ASCE, 2478-2490

Kamphuis, J.W., Davies, M.H., Nairn, R.B. and Sayao, O.J. (1986), "Calculation of Littoral Sand Transport Rate," Coastal Engineering. 10, 1-21.

Komar, P.D. (1988), "Environmental Controls on Littoral Sand Transport," Proceedings 21st International Conference On Coastal Engineering, ASCE, 1238-1252.

Komar, P.D. (1990), "Littoral Sediment Transport," In: Herbich, J.B (Ed), Handbook Of Coastal And Ocean Engineering, Chap. 25, Vol II. Gulf Pub., Houston, TX.

Komar, P.D. and Inman, D.L., (1970), "Longshore Sand Transport On Beaches," Journal of Geophysical Research, 75(30), 5914 – 5927.

Komar, P.D., (1998), "Beach Processes and Sedimentation," 2nd Edn. Prentice-Hall, Upper Saddle River, NJ.

Kraus, N.C., and Dean, J.L. (1987), "Longshore Sediment Transport Rate Distribution," Proceedings Coastal Sediments '87, ASCE, 881-896.

Kraus, N.C., Ginger, K.J., and Rosati, J.D. (1988), "Toward An Improved Empirical Formula For Longshore Sand Transport," Coastal Engineering '98 - Chapter 88:1184-1196.

Kraus, N.C., Ginger, K.J., and Rosati, J.D. (1988), "Toward an Improved Empirical Formula For Longshore Sand Transport," Proceedings 21st International Conference On Coastal Engineering, 1184-1196.

Kraus, N.C., Gingerinch, K.J., and Rogati, J.P., (1989), "Duck 85 Surf Zone Sand Transport Experiment," U.S. Army Engineer Waterways Experiment Station, Technical Report CERC-89-5, Vicksburg, Mississippi.

Kriebel, D.L., Kraus, N.C., and Larson, M., (1991), "Engineering Methods For Predicting Beach Profile Response," Proceedings Coastal Sediments '91, ASCE, 557-571.

Larson, M. and Bayram, A. (2005), "Calculating Cross-Shore Distribution of Longshore Sediment Transport," In: Port and Coastal Engineering, Developments in Sciecne and Technology, Editor P. Bruun, Journal of Coastal Research Special Issue No. 46, 203-235.

Larson, M., Kraus, N.C., and Hanson, H. 2002. "Simulation of Regional Longshore Sediment Transport and Coastal Evolution – The Cascade Model," Proceedings 28th International Conference On Coastal Engineering, World Scientific, 2612-2624.

Masselink, G., and Hughes, M.G. (2003), "Introduction To Coastal Processes and Geomorphology," Published by Holder Arnold, Holder Headline Group, 338 Eustorn Road, London.

Miller, H.C., (1998), "Comparison of Storm Longshore Transport Rates To Predictions," Proceedings 26th Conference On Coastal Engineering, ASCE, 2954-2967.

Miller, H.C. (1999), "Field Measurements of Longshore Sediment Transport During Storm," Coastal Engineering, 36, 301-321.

Rosati, J.D. And Kraus, N.C., (1989), "Development Of A Portable Sand Trap for Use in the Nearshore," Technical Report CERC-8-9, U.S. Army Corps Of Engineers, Waterways Experiment Station, Coastal Engineering Research Center, Vicksbug, Mississipi.

Schoonees, J.S. (2001), "Longshore Sediment Transport: Applied Wave Power Approach, Field Data Analysis And Evaluation of Formulae," Dissertation of Doctor of Philosophy, University of Stellenbosch., Published by CSIR, Pretoria, Republic of South Africa.

Schoonees, J.S., & Theron, A.K. (1993), "Review of the Field-Data Base for Longshore Sediment Transport," Coastal Engineering, 19, 1-25.

Smith, E.R., Wang, P. and Zhang. J. (2003), “Evaluation of the CERC Formula Using Large-Scale Model Data,” U.S. Army Engineer Research and Development Center, Coastal and Hydraulics Laboratory, Vicksburg.

Sorensen, R.B. (1994), “Basic Wave Mechanics for Coastal and Ocean Engineers,” Wiley-Interscience Publications, John Wiley & Sons, Inc.

Sternberg, R.W., Shi, N.C. and Downing, J.P., (1984), “Field Investigation of Suspended Sediment Transport In The Nearshore Zone,” Proceedongs 19th International Conference On Coastal Engineering, ASCE, 1782 – 1798.

Swart, D.H. (1976), “Predictive Equations Regarding Coastal Transport,” Proceedings 15th International Conference On Coastal Engineering, ASCE, 1113-1132.

US Army Corps of Engineers, (1984), “Shore Protection Manual,” Vols. I and II., Coastal Engineering Research Center, WES Vickburg, MS.

US Army Corps of Engineers, (2002), “Coastal Engineering Manual,” Engineer Manual 1110-2-1100, Washington, D.C.

Wang, P. and Kraus, N.C., (1999), “Longshore Sediment Transport Rate Measurement by Short-Term Impoundment,” Journal Of Waterway, Port, Coastal And Ocean Engineering, 125, 118 – 125.

Wang, P., Kraus, N.C., and Davis, R.A.Jr. (1998), “Total Longshore Sediment Transport Rate in the Surf Zone: Field Measurements and Empirical Predictions,” Journal of Coastal Research, 14(1), 269-282.

Wellen, E.V., Chadwick, A.J., and Mason, T. (2000), “A Review and Assessment of Longshore Sediment Transport Equations for Coarse-Grained Beaches,” Coastal Engineering, 243-275.

Yu, Y., Stenberg, R.W. and Beach, R.A, (1993), “Kinematics of Breaking Waves and Associated Suspended Sediment in The Nearshore Zone,” Continental Shelf Research, 13(11), 1219 – 1242.

Internet Sources

http://en.wikipedia.org/wiki/Longshore_drift,

http://www.fortunecity.com/greenfield/ecolodge/25/spurn.htm,

http://geology.about.com/library/bl/images/bltombolo.htm,

http://web.engr.oregonstate.edu/~scottc2/pdf/Smith_2003.pdf

http://www.environmentaltracing.info.

http://www.fortunecity.com/greenfield/ecolodge/25/spurn.htm

http://geology.about.com/library/bl/images/bltombolo.htm

APPENDIX A

REVIEW OF ORIGINAL DATA SETS – LABORATORY AND FIELD DATA

Table A.1 Laboratory Data Set – LSTF, (Smith *et al*., 2002)

Experiment Number	Breaker Type	H_{mo} (m)	H_{sb} (m)	T_p (s)	h (m)	α_b (degree)	$\sin 2\alpha_b$	$\cos \alpha$	γ_b	$Q_{measured}$ (m^3/s)
1	Spilling	0.25	0.26	1.5	0.9	6.5	0.224951054	0.993571885	0.57	0.00008552
3	Plunging	0.23	0.27	3	0.9	6.4	0.221548497	0.993767919	0.96	0.00022634
5	Spilling	0.16	0.18	1.5	0.9	6.7	0.231747903	0.985703469	0.29	0.000037616
6	Plunging	0.19	0.21	3	0.9	6.4	0.221548497	0.993767919	0.58	0.00010963

Table A.2 Field Data Data Set – DUCK85, (Kraus *et al.*, 1986)

Date	Profile Type	H_{rms} (m)	T_p (m)	D_{ref} (m)	X_b (m)	V_{mean} (m/s)	H_b (m)	I** (N/s)	$Q_{measured}$ (m^3/s)
Sept. 5, 1985, 0975	Shelf	0.5	11.4	2.14	35.1	0.11	1.06	2.71	0.000283
Sept. 5, 1985, 1075	Shelf	0.46	11.2	1.8	33.7	0.17	0.97	2.95	0.000308
Sept. 5, 1985, 1352	Shelf	0.54	10.9	2.19	32.8	0.17	1.19	5.47	0.000572
Sept. 5, 1985, 1528	Shelf	0.46	11.1	1.94	42.1	0.22	0.96	17.81	0.00186
Sept. 6, 1985, 0916	Shelf	0.48	12.8	1.4	38.2	0.3	0.86	19.43	0.00203
Sept. 6, 1985, 1018	Shelf	0.36	13.1	2.14	36.5	0.29	0.83	6.92	0.000723
Sept. 6, 1985, 1303	Shelf	0.42	10.1	2.34	27.9	0.22	0.88	3.25	0.00034
Sept. 6, 1985, 1400	Shelf	0.36	11.2	2.34	33.1	0.18	0.85	3.79	0.000396

Table A.3 Field Data Data Set – SANDYDUCK 1 (Storm Conditions), (Miller, 1999)

Storm Date	Waves Height, H_{mo} (m)	Waves Period (s)	Waves Direction (deg)	$Q_{measured}$ (m^3/h)-North Side	$Q_{measured}$ (m^3/s)-North Side
11-Nov-95	1.9	7.6	14	530	0.14722222
11-Mar-96	2.8	7	10	1780	0.49444444
12-Mar-96	3.5	12	14	450	0.125
27-Mar-96	1.8	6.7	25	560	0.15555556
02-Apr-96	1.6	7	26	670	0.18611111

Table A.4 Field Data Data Set – SANDYDUCK 2, (Miller, 1998)

Date	Profile Type	H_{rms} (m)	T_p (m)	D_{ref} (m)	V_{mean} (m/s)	Temp (deg)	D_{50} (mm)	w (m/s)	$Q_{measured}$ (m^3/yr)	$Q_{measured}$ (m^3/s)
March 31, 1997	Bar	1.36	8	6.7	0.49	15	0.165	0.019264	4625534	0.148711866
April 1, 1997	Bar	2.92	8	6.82	1.1	15	0.165	0.019264	27323564	0.878458202
October 20, 1997	Bar	2.27	12.8	6.44	0.53	15	0.165	0.019264	6889513	0.221499274
February 04, 1998	Bar	3.18	12.8	8.59	0.6	15	0.165	0.019264	10580828	0.340175792
February 05, 1998	Bar	2.94	12.8	6.83	0.45	15	0.165	0.019264	9298562	0.298950687

Table A.5 Field Data Data Set – Compiled by Schoonees and Theron (1993).

Location	D50	θ_b (deg)	sin $2\theta_b$	cos θ_b	H_{bs} (m)	T_p (s)	$Q_{measured}$ Q (m^3/yr)	$Q_{measured}$ Q (m^3/s)
El Moreno	0.6	10	0.3420	0.9848	0.45	2.7	146475	0.004709
El Moreno	0.6	14	0.4695	0.9703	0.56	3.3	274293	0.008819
El Moreno	0.6	9.6	0.3289	0.9860	0.39	5.2	47436	0.001525
El Moreno	0.6	10.9	0.3714	0.9995	0.51	4.3	139131	0.004473
El Moreno	0.6	2.5	0.0872	0.9990	0.4	6.6	19848	0.000638

El Moreno	0.6	7.4	0.2554	0.9917	0.41	5.3	29176	0.000938
El Moreno	0.6	4	0.1392	0.9976	0.4	3.8	67482	0.002170
Silver Strand	0.175	0.3	0.0105	1.0000	1.27	12	41680	0.001340
Silver Strand	0.175	4.4	0.1530	0.9971	1.46	11.3	981263	0.031548
Silver Strand	0.175	5.8	0.2011	0.9949	0.75	11.1	153025	0.004920
Silver Strand	0.175	4.3	0.1495	0.9972	0.8	9.5	123055	0.003956
Leadbetter	0.22	4.2	0.1461	0.9973	0.7	10.8	250000	0.008038
Leadbetter	0.22	3.2	0.1115	0.9984	0.85	11.1	466000	0.014982
Leadbetter	0.22	5.6	0.1942	0.9952	0.78	12.4	348920	0.011218
Leadbetter	0.22	8	0.2756	0.9903	1.77	11.9	3904608	0.125534
Leadbetter	0.22	3.8	0.1323	0.9978	0.76	8	71000	0.002283
Leadbetter	0.22	6.2	0.2147	0.9942	0.65	7.2	99000	0.003183
Leadbetter	0.22	5.7	0.1977	0.9951	0.69	11.4	248000	0.007973
Leadbetter	0.22	5.9	0.2045	0.9947	0.75	11.2	241000	0.007748
Torrey Pines	0.2	3.4	0.1184	0.9982	1.12	13.4	487456	0.015672
Torrey Pines	0.157	3.4	0.1184	0.9982	1.29	13.4	1166339	0.037498
Duck	0.46	16.5	0.5446	0.9588	1.99	7	8150000	0.262024
Duck	0.46	5	0.1736	0.9962	0.88	12	140000	0.004501
Lake Worth	0.42	16.8	0.5534	0.9573	0.55	6.9	95647	0.003075
Lake Worth	0.42	11.5	0.3907	0.9799	0.46	4.9	75582	0.002430
Lake Worth	0.42	15.5	0.5150	0.9636	0.28	7.5	26882	0.000864
Channel Islands	0.22	3.1	0.1080	0.9985	0.84	12.6	469791	0.015104
Channel Islands	0.22	3.1	0.1080	0.9985	1.09	11.8	556327	0.017886
Channel Islands	0.22	3	0.1045	0.9986	1.27	11.3	1427237	0.045886
Channel Islands	0.22	3.2	0.1115	0.9984	1.27	11.5	1304182	0.041930
Channel Islands	0.22	3.1	0.1080	0.9985	1.14	12	798665	0.025677
Channel Islands	0.22	2.8	0.0976	0.9988	1.67	11.1	1059859	0.034075
Price Inlet	0.25	9	0.3090	0.9877	0.85	9.5	227453	0.007313
Price Inlet	0.25	4	0.1392	0.9976	0.92	8.9	79192	0.002546
Price Inlet	0.18	5	0.1736	0.9962	0.79	8.3	213957	0.006879
Price Inlet	0.18	9	0.3090	0.9877	0.99	9.2	454112	0.014600
Pointe Sapin	0.58	9.3	0.3190	0.9869	1	8.6	1440000	0.046296

Pointe Sapin	0.58	10.9	0.3714	0.9820	0.74	7.25	550000	0.017683
Anaheim Bay	0.4	21	0.6691	0.9336	0.494	13.7	327000	0.010513
Anaheim Bay	0.4	9	0.3090	0.9877	1.026	13.7	595000	0.019129
Anaheim Bay	0.4	21	0.6691	0.9336	0.338	13.7	85000	0.002733
Anaheim Bay	0.4	21	0.6691	0.9336	0.654	13.7	173000	0.005562
Anaheim Bay	0.4	21	0.6691	0.9336	0.612	13.7	469000	0.015078
Pt. Mugu	0.154	15	0.5000	0.9659	1.1	16.6	2400000	0.077160
Lake Michigan	0.5	12	0.4067	0.9781	0.254	4	94692	0.003044
Lake Michigan	0.5	10	0.3420	0.9848	0.356	3.5	74566	0.002397
Lake Michigan	0.43	13	0.4384	0.9744	0.28	2.5	64008	0.002058
Lake Michigan	0.5	5	0.1736	0.9962	0.585	3.8	68297	0.002196
Lake Michigan	0.23	16	0.5299	0.9613	0.204	3.3	35963	0.001156
Lake Michigan	0.285	6	0.2079	0.9945	0.176	3	5939	0.000191
Lake Michigan	0.32	27	0.8090	0.8910	0.076	4	8578	0.000276
Cape Thompson	1	25	0.7660	0.9063	1.676	5.5	1310000	0.042117
Cotonou	0.4	9	0.3090	0.9877	1.4	12	1200000	0.038580
Safi (Maroc)	0.5	10.4	0.3551	0.9836	3.4	12	14793000	0.475598
Agadir (")	0.17	4.2	0.1461	0.9973	2.1	12	3409000	0.109600
Agadir (")	0.2	5	0.1736	0.9962	3	12	4261000	0.136992
Pt. Noire	0.3	1.9	0.0663	0.9995	1.9	12	600000	0.019290
Lome (Benin)	0.19	4.9	0.1702	0.9963	1.6	11	1250000	0.040188
Ventnor	0.2	6.4	0.2215	0.9938	0.45	7.5	120000	0.003858
Nags Head	0.29	6.4	0.2215	0.9938	0.6	8.5	420000	0.013503
Ivory Coast	0.5	4.5	0.1564	0.9969	3	12	1000000	0.032150
DUCK	0.2	6.5	0.2250	0.9936	0.52	9	37000	0.001190
DUCK	0.2	6.5	0.2250	0.9936	0.52	9	45000	0.001447
DUCK	0.193	5.5	0.1908	0.9954	0.6	9	64000	0.002058
DUCK	0.193	5.5	0.1908	0.9954	0.6	9	79000	0.002540
DUCK	0.84	5.5	0.1908	0.9954	0.45	8.2	118000	0.003794
DUCK	0.84	5.5	0.1908	0.9954	0.45	8.2	174000	0.005594
Miyazu	0.32	5	0.1736	0.9962	0.058	6	700	0.000023
Miyazu	0.32	5	0.1736	0.9962	0.064	6	600	0.000019

Miyazu	0.32	5	0.1736	0.9962	0.073	6	900	0.000029
Miyazu	0.32	5	0.1736	0.9962	0.148	6	1000	0.000032
Miyazu	0.32	5	0.1736	0.9962	0.193	6	1200	0.000039
Miyazu	0.32	5	0.1736	0.9962	0.351	6	8800	0.000283
Miyazu	0.32	5	0.1736	0.9962	0.382	6	6600	0.000212
Miyazu	0.32	5	0.1736	0.9962	0.442	6	9000	0.000289
Rosseika	0.35	12	0.4067	0.9781	1.12	4.8	190933	0.006139
Rosseika	0.26	15	0.8660	0.9659	0.84	4.3	27787	0.000893
Rosseika	0.25	10	0.3420	0.9848	0.56	4	57161	0.001838
Rosseika	0.25	15	0.8660	0.9659	0.653	3.8	58947	0.001895
Rosseika	0.22	15	0.8660	0.9659	0.933	4.6	112139	0.003605
Rosseika	0.32	10	0.3420	0.9848	0.746	5.7	51405	0.001653
Rosseika	0.36	10	0.3420	0.9848	0.653	3.8	26993	0.000868
Primorskoe	0.43	30	0.8660	0.8660	1.493	6	887185	0.028523
Primorskoe	0.4	15	0.8660	0.9659	0.84	4.2	256033	0.008232
Primorskoe	0.39	10	0.3420	0.9848	1.4	5.2	601381	0.019335
Primorskoe	0.33	25	0.7660	0.9063	1.773	6.8	1784294	0.057365
Primorskoe	0.34	18	0.5878	0.9511	1.493	5.4	750237	0.024120
Primorskoe	0.25	10	0.3420	0.9848	0.933	4.8	222293	0.007147
Rosseika	0.36	25	0.7660	0.9063	1.586	5.9	869323	0.027949
Rosseika	0.3	5	0.1736	0.9962	0.84	5.1	103207	0.003318
Rosseika	0.36	25	0.7660	0.9063	0.933	5.8	146872	0.004722
Rosseika	0.32	18	0.5878	0.9511	0.746	5.9	134566	0.004326
Rosseika	0.28	20	0.6428	0.9397	0.746	4.2	183590	0.005902
Rosseika	0.3	10	0.3420	0.9848	0.933	3.8	149452	0.004805
Rosseika	0.28	5	0.1736	0.9962	1.12	5	76413	0.002457
Rosseika	0.4	5	0.1736	0.9962	0.84	4.2	30764	0.000989
Rosseika	0.37	5	0.1736	0.9962	1.12	6.2	37512	0.001206
Rosseika	0.28	20	0.6428	0.9397	1.493	5.8	1063829	0.034202
Rosseika	0.28	30	0.8660	0.8660	1.12	5.3	593442	0.019079
Rosseika	0.29	5	0.1736	0.9962	0.746	4.1	40092	0.001289
Rosseika	0.32	10	0.3420	0.9848	0.933	5.4	89711	0.002884

Kinburn	0.55	30	0.8660	0.8660	1.4	4.5	1569941	0.050474
Kinburn	0.7	35	0.9397	0.8192	0.746	4.3	104200	0.003350
Kinburn	0.3	10	0.3420	0.9848	0.56	4	8137	0.000262
Kinburn	0.28	20	0.6428	0.9397	0.653	4.1	35150	0.001130
Kinburn	0.48	15	0.8660	0.9659	0.933	5.9	62520	0.002010
Kinburn	0.5	15	0.8660	0.9659	0.746	3.6	34932	0.001123
Kinburn	0.47	10	0.3420	0.9848	0.56	4.3	13893	0.000447
Kinburn	0.28	10	0.3420	0.9848	0.746	3.8	39298	0.001263
Kinburn	0.32	10	0.3420	0.9848	1.306	4.7	377103	0.012124
Kinburn	0.23	20	0.6428	0.9397	1.773	5.7	1633453	0.052516
Kinburn	0.24	20	0.6428	0.9397	0.653	3.3	45252	0.001455
Kinburn	0.22	30	0.8660	0.8660	0.84	4.2	305652	0.009827
Kinburn	0.23	25	0.7660	0.9063	1.306	4.7	843521	0.027119
Shoreham	0.15	12.5	0.4226	0.9763	0.31	2.32	1490	0.000048
Shoreham	0.15	13	0.4387	0.9744	0.33	2.32	1900	0.000061
Shoreham	0.15	18.5	0.6018	0.9483	0.37	2.79	9436	0.000303
Shoreham	0.15	20	0.6428	0.9397	0.45	2.9	7511	0.000241
Shoreham	0.15	13	0.4384	0.9744	0.33	2.42	2174	0.000070
Shoreham	0.15	14	0.4695	0.9703	0.6	3	11739	0.000377
Shoreham	0.15	9	0.3090	0.9877	0.9	2.9	8710	0.000280
Portugal	0.38	10	0.3420	0.9848	1.2	10	210000	0.006752
Lobito	0.45	25	0.7660	0.9063	0.65	10	200000	0.006430

Table A.6 Field Data Data Set – Wang *et al.* (1998)

Location	H_{rms} (m)	Wave Height (deg)	sin $2\alpha_b$	cos α_b	Wave Period (s)	Grain Size (mm)	$Q_{measured}$ (m^3/yr)	$Q_{measured}$ (m^3/s)
Emerald Isle, NC	0.79	13.5	0.4540	0.9724	7.5	0.35	110000	0.003537
Onslow Beach, NC	0.61	12	0.4067	0.9781	6	2.25	42000	0.001350
Myrtle Beach, SC	0.51	4	0.1392	0.9976	8.5	0.26	6000	0.000193
Jekyll Island, GA	0.2	3	0.1045	0.9986	3.5	0.17	2000	0.000064

Jekyll Island, GA	0.35	10	0.3420	0.9848	3.3	0.26	52000	0.001672
Anastacia Beach, FL	0.49	5.5	0.1908	0.9954	10.5	0.19	8000	0.000257
N. Mantazas Beach, FL	0.44	7.2	0.2487	0.9921	7.2	0.28	12000	0.000386
Canaveral Seashore, FL	0.46	9	0.3090	0.9877	3.5	0.9	19000	0.000611
Melbourne Beach, FL	0.5	2.5	0.0872	0.9990	3.5	1.5	6000	0.000193
Beverly Beach, FL	0.36	11.5	0.3907	0.9799	3.5	0.41	10000	0.000322
Lido Key Beach, FL	0.38	14	0.4695	0.9703	3.7	0.68	39000	0.001254
Lido Key Beach, FL	0.34	19	0.6157	0.9455	3.4	0.54	37000	0.001190
Lido Key Beach, FL	0.21	2.6	0.0906	0.9990	3	0.37	1000	0.000032
St. George Island, FL	0.29	35.3	0.9432	0.8161	3	0.29	45000	0.001447
St. George Island, FL	0.22	31.5	0.8910	0.8526	2.9	0.41	3000	0.000096
St. George Island, FL	0.28	23	0.7719	0.9205	3	0.43	6000	0.000193
St. Joseph Island, FL	0.53	9.3	0.3190	0.9869	4.2	0.24	56000	0.001800
Grayton Beach, FL	0.56	8.5	0.2924	0.9890	4.5	0.28	60000	0.001929
Redington Beach, FL	0.36	8.4	0.2890	0.9893	4.5	0.85	15000	0.000482
Redington Beach, FL	0.28	10.7	0.3649	0.9826	3.9	0.2	6000	0.000193
Redington Beach, FL	0.32	19.2	0.6211	0.9444	4.5	0.9	8000	0.000257
Redington Beach, FL	0.24	15.8	0.5240	0.9622	4.9	0.43	5000	0.000161
Redington Beach, FL	0.69	13.1	0.4415	0.9740	7.3	0.37	145000	0.004662
Indian Shores, FL	0.36	20	0.4628	0.9397	4.5	0.32	34000	0.001093
Indian Shores, FL	0.31	1.8	0.0628	0.9995	3.3	0.4	1000	0.000032
Indian Rocks Beach, FL	0.36	7.7	0.2656	0.9910	2.9	0.28	19000	0.000611
Indian Rocks Beach, FL	0.34	7.5	0.2588	0.9914	4.2	0.42	23000	0.000739
Indian Rocks Beach, FL	0.19	10	0.3420	0.9848	2.8	1.38	3000	0.000096
Indian Rocks Beach, FL	0.14	8.2	0.0282	0.9898	3.8	1.29	2000	0.000064

APPENDIX B

CALCULATION OF LONGSHORE SEDIMENT TRANSPORT RATE

B.1 Laboratory Database: Large-Scale Sediment Transport Facility (LSTF), (Smith *et al.*, 2002)

[A] Calculation of the Group Velocity *Cgb*:

$$C_{gb} = \sqrt{g \frac{H_b}{\gamma}}, [m/s]$$

where :

g	=	9.81	[m/s^2]

[B] Calculation of the Average Longshore Current V_m :

$$V_m = \frac{1}{x_b} \int_0^{x_b} V dx = \frac{5}{64} \frac{\pi \gamma \sqrt{g}}{c_f} A^{3/2} \sin 2\alpha_b, [m/s]$$

where :

π	=	3.142	[dimensionless]
g	=	9.81	[m/s^2]
c_f	=	0.005	[dimensionless]

and :

$$A = \frac{9}{4} \left(\frac{w^2}{g} \right)^{1/3}, [m^{1/3}]$$

In these experiments, the grain size was estimated to 0.15mm. If we assume that the temperature is 20 deg, this gives the fall velocity w = 0.018279 m/s. Using the formula for A, gives :

A	=	0.0729	[$m^{1/3}$]

For this case, the A value will be the same.

[C] Calculation of the Wave Energy Flux F :

$$F = \frac{1}{8}\rho g H_b^2 C_{gb} \cos\alpha_b, [Nm/m^2]$$

where :

ρ	=	1000	[kg/m^3]
g	=	9.81	[m/s^2]

[D] Calculation of the Total Longshore Sediment Transport Rate K or Q/ε :

The newly derived formula :

$$Q = \frac{\varepsilon}{(\rho_s - \rho)(1-a)gw} FV, [m^3/s]$$

where :

ρ	=	1000	[kg/m^3]
g	=	9.81	[m/s^2]
ρ_s	=	2650	[kg/m^3]
a	=	0.4	[dimensionless]
w	=	0.0182	[m/s]

and :

$$\text{Const} = \frac{1}{(\rho_s - \rho)(1-a)gw} = 0.0056$$

The result is,

			[A]			[B]		[C]	[D]		
Experiment Number	H_{sb}	γ_b	C_{gb}	α_b	$\sin 2\alpha_b$	V_m	$\cos \alpha_b$	F	K	$Q_{measured}$ (m^3/s)	$\varepsilon = Q_{measured}/K$
	[m]	[-]	[m/s]	[deg]	[-]	[m/s]	[-]	[Nm/m^2]	[m^3/s]		[-]
1	0.26	0.57	*2.1154*	6.5	0.2250	*0.3885*	0.9936	*174.2243*	*0.3813*	8.55E-05	*2.24E-04*
3	0.27	0.96	*1.6610*	6.4	0.2215	*0.6445*	0.9938	*147.5612*	*0.5357*	2.26E-04	*4.23E-04*
5	0.18	0.29	*2.4676*	6.7	0.2317	*0.2037*	0.9857	*96.6367*	*0.1109*	3.76E-05	*3.39E-04*
6	0.21	0.58	*1.8846*	6.4	0.2215	*0.3894*	0.9938	*101.2821*	*0.2222*	1.10E-04	*4.93E-04*
									Mean		**0.00037**
									Standard deviation		**0.0001**

B.2 Field Database : DUCK85 Surf Zone Sand Transport Experiment, (Kraus *et al.*, 1989)

[A] Calculation of the Group Velocity C_{gb} :

$$C_{gb} = \sqrt{g\frac{H_b}{\gamma}}, [m/s]$$

where :

g = 9.81 [m/s^2]

γ = 0.78 [dimensionless]

Since there was no information about the breaker index γ, the value of 0.78 was used.
In the DUCK85 experiments, the average longshore current V_m was measured. Therefore, there is no need to calculate V_m; instead we can use the measured values directly. In addition, the value of A is not important.

[B] Calculation of the Wave Energy Flux F :

$$F = \frac{1}{8}\rho g H_b^2 C_{gb} \cos\alpha_b, [Nm/m^2]$$

where :

ρ	=	1000	[kg/m^3]
g	=	9.81	[m/s^2]

There was no information about the wave angle at breaking point; therefore, an assumption was made that the angle is small at wave breaking. This gives the value of $cos\ \alpha_b$ is 1.0.

[C] Calculation of the Total Longshore Sediment Transport Rate K or Q/ε :

The newly derived formula :

$$Q = \frac{\varepsilon}{(\rho_s - \rho)(1-a)gw} FV, [m^3/s]$$

where :

ρ	=	1025	[kg/m^3]
g	=	9.81	[m/s^2]
ρ_s	=	2650	[kg/m^3]
a	=	0.4	[dimensionless]
w	=	0.019264	[m/s]

In these experiments, the grain size was measured to be 0.165mm. We assume that the temperature is 15 deg and this gives the fall velocity w = 0.019264 m/s.

and :

$$\text{Const} = \frac{1}{(\rho_s - \rho)(1-a)gw} = 0.005427$$

The result is,

				[A]	[B]	[C]		
Date		V_{mean} [m/s]	H_b [m]	C_{gb} [m/s]	F [Nm/m^2]	K [m^3/s]	$Q_{measured}$ [m^3/s]	ε = Qmeasured/K [-]
Sept. 5, 1985, 0975		0.11	1.06	*3.6512*	*5156.4968*	*3.0784*	0.000283	*9.19309E-05*
Sept. 5, 1985, 1075		0.17	0.97	*3.4928*	*4130.6598*	*3.8111*	0.000308	*8.08174E-05*
Sept. 5, 1985, 1352		0.17	1.19	*3.8687*	*6885.8489*	*6.3531*	0.000572	*9.00351E-05*
Sept. 5, 1985, 1528		0.22	0.96	*3.4747*	*4025.0212*	*4.8058*	0.00186	*0.00038703*
Sept. 6, 1985, 0916		0.3	0.86	*3.2888*	*3057.2870*	*4.9778*	0.00203	*0.000407813*
Sept. 6, 1985, 1018		0.29	0.83	*3.2309*	*2797.5981*	*4.4031*	0.000723	*0.000164202*
Sept. 6, 1985, 1303		0.22	0.88	*3.3268*	*3238.1486*	*3.8663*	0.00034	*8.79391E-05*
Sept. 6, 1985, 1400		0.18	0.85	*3.2696*	*2969.1860*	*2.9006*	0.000396	*0.000136524*
						Mean		**0.000180786**
						Standard deviation		**0.000127993**

B.3 Field Database : SANDYDUCK 1 Surf Zone Sand Transport Experiment (Storm Conditions), (Miller, 1999)

In the SANDYDUCK 1 experiments, (Miller, 1999), the wave height at breaking, wave angle at breaking and the mean longshore current velocity were not measured. In that case, the wave properties at breaking need to be calculated. It was assumed that the original input wave conditions were in deep water. So, the wave properties at breaking can be calculated by solving the energy wave flux equation and Snell's law.

[a] The Energy Wave Flux :

$$H_o^2 C_{go} \cos\alpha_o = H_b^2 C_{gb} \cos\alpha_b$$

and,

[b] Snell's Law :

$$\frac{\sin\alpha_o}{C_o} = \frac{\sin\alpha_b}{C_b}$$

where :

For group velocity in deep water:

$$C_o = C_{go} = \frac{gT}{4\pi}$$

For group velocity in shallow water (break point):

$$C_b = C_{gb} = \sqrt{g\frac{H_b}{\gamma}}$$

Assume that γ is 0.78 and g is 9.81 m/s^2.

The input wave properties in deep water are given below :

Date	Wave Height, H_o	Wave Period, T_p	Wave Direction, α_o
	[m]	[s]	[deg]
11-Nov-95	1.9	7.6	14
11-Mar-96	2.8	7	10
12-Mar-96	3.5	12	14
27-Mar-96	1.8	6.7	25
02-Apr-96	1.6	7	26

After using both equations (energy wave flux and Snell's law), the input wave properties at breaking were obtained as :

Date	Wave Height, H_b	Wave Period, T_p	Wave Direction, α_b
	[m]	[s]	[deg]
11-Nov-95	2.1	7.6	12.1
11-Mar-96	2.7	7	10.7
12-Mar-96	4	12	10.6
27-Mar-96	1.9	6.7	23.3
02-Apr-96	1.7	7	21.8

The properties at wave breaking were used in the next calculations.

[A] Calculation of the Group Velocity C_{gb} :

$$C_{gb} = \sqrt{g \frac{H_b}{\gamma}}, [m/s]$$

where :

g	=	9.81	[m/s^2]
γ	=	0.78	[dimensionless]

Since there was no information obtained about breaker index γ, the value of 0.78 is used.

[B] Calculation of the Average Longshore Current V_m :

$$V_m = \frac{1}{x_b}\int_0^{x_b} V dx = \frac{5}{64}\frac{\pi\gamma\sqrt{g}}{c_f} A^{3/2} \sin 2\alpha_b, [m/s]$$

where :

π	=	3.142	[dimensionless]
g	=	9.81	[m/s^2]
c_f	=	0.005	[dimensionless]
γ	=	0.78	[dimensionless]

and :

$$A = \frac{9}{4}\left(\frac{w^2}{g}\right)^{1/3}, [m^{1/3}]$$

In these experiments, the grain size was estimated to 0.165mm. If we assume that the temperature is 15 deg, this gives the fall velocity w = 0.019264 m/s. Using the formula for A, gives :

A	=	0.07556	[m$^{1/3}$]

This value was employed when calculating the longshore velocity.

[C] Calculation of the Wave Energy Flux F :

$$F = \frac{1}{8}\rho g H_b^2 C_{gb} \cos\alpha_b, [Nm/m^2]$$

where :

ρ	=	1025	[kg/m^3]
g	=	9.81	[m/s^2]

[D] Calculation of the Total Longshore Sediment Transport Rate K or Q/ε :

The newly derived formula :

$$Q = \frac{\varepsilon}{(\rho_s - \rho)(1-a)gw} FV, [m^3/s]$$

where :

ρ	=	1025	[kg/m^3]
g	=	9.81	[m/s^2]
ρ_s	=	2650	[kg/m^3]
a	=	0.4	[dimensionless]
w	=	0.019264	[m/s]

and :

Const = $\frac{1}{(\rho_s - \rho)(1-a)gw} = 0.005427$

The result is,

		[A]			[B]		[C]	[D]		
Date	H_b	C_{gb}	α_b	$\sin 2\alpha_b$	V_m	$\cos \alpha_b$	F	K or Q/ε	$Q_{measured}$	$\varepsilon = Q_{measured}/K$
	[m]	[m/s]	[deg]	[-]	[m/s]	[-]	[Nm/m^2]	[m^3/s]	[m^3/s]	[-]
11-Nov-95	2.1	5.1392	12.1	0.4099	1.0210	0.9778	27854.05	154.3506	0.1472	0.000954
11-Mar-96	2.7	5.8273	10.7	0.3649	0.9089	0.9826	52465.8	258.8166	0.4944	0.00191
12-Mar-96	4	7.0928	10.6	0.3616	0.9007	0.9829	140200.4	685.3618	0.125	0.000182
27-Mar-96	1.9	4.8884	23.3	0.7242	1.8039	0.9184	20370.7	199.4374	0.1556	0.00078
02-Apr-96	1.7	4.6239	21.8	0.6896	1.7178	0.9285	15595.32	145.3897	0.1861	0.00128
								Mean		**0.001021**
								Standard deviation		**0.00057**

B.4 Field Database : SANDYDUCK 2 Surf Zone Sand Transport Experiment, (Miller, 1998)

[A] Calculation of the Group Velocity C_{gb} :

$$C_{gb} = \sqrt{g \frac{H_b}{\gamma}}, [m/s]$$

where :

g	=	9.81	[m/s^2]
γ	=	0.78	[dimensionless]

Since there was no information obtained about breaker index γ, the value of 0.78 is used.

In SANDYDUCK 2 experiments, the data of the average longshore current velocity V_m were measured. In that case, there is no need to calculate *Vm*; instead we can use the measured values directly. In addition, the value of *A* is not important.

[B] Calculation of the Wave Energy Flux *F* :

$$F = \frac{1}{8}\rho g H_b^2 C_{gb} \cos\alpha_b, [Nm/m^2]$$

where :

ρ	=	1025	[kg/m^3]
g	=	9.81	[m/s^2]

There was no information about wave angle at the break point; therefore, and an assumption was made that the angle is small at the break point. This gives the value of $cos\ \alpha_b = 1.0$.

[C] Calculation of the Total Longshore Sediment Transport Rate *K* or *Q*/ε :

The newly derived formula :

$$Q = \frac{\varepsilon}{(\rho_s - \rho)(1-a)gw} FV, [m^3/s]$$

where :

ρ	=	1025	[kg/m^3]
g	=	9.81	[m/s^2]
ρ_s	=	2650	[kg/m^3]
a	=	0.4	[dimensionless]
w	=	0.019264	[m/s]

In these experiments, the grain size has been identified to 0.165mm. Assume that the temperature is 15 deg, this gives the fall velocity w = 0.019264 m/s. So,

$$\text{Const} = \frac{1}{(\rho_s - \rho)(1-a)gw} = 0.005427$$

The result is,

Date		H_{rms} [m]	[A] C_{gb} [m/s]	V_m [m/s]	[B] F [Nm/m^2]	[C] Q/ε or K [m^3/s]	$Q_{measured}$ [m^3/s]	$\varepsilon = Q_{measured}/K$ [-]
March 31, 1997		1.36	*4.1358*	0.49	*9614.7359*	*25.5688*	0.148712	0.0058161
April 1, 1997		2.92	*6.0601*	1.1	*64945.2237*	*387.7194*	0.878458	0.0022657
October 20, 1997		2.27	*5.3432*	0.53	*34606.2652*	*99.5424*	0.221499	0.0022252
February 04, 1998		3.18	*6.3241*	0.6	*80381.8298*	*261.7501*	0.340176	0.0012996
February 05, 1998		2.94	*6.0808*	0.45	*66063.0186*	*161.3424*	0.298951	0.0018529
						Mean		**0.0026919**
						Standard deviation		**0.00160017**

B.5 Field Database : Compilation of Longshore Sediment Transport provided by Schoonees and Theron, 1993.

[A] Calculation of the Group Velocity C_{gb} :

$$C_{gb} = \sqrt{g\frac{H_b}{\gamma}}, [m/s]$$

where :

g	=	9.81	[m/s^2]
γ	=	0.78	[dimensionless]

Since there was no information about breaker index γ, the value of 0.78 is used.

[B] Calculation of the Average Longshore Current V_m :

$$V_m = \frac{1}{x_b}\int_0^{x_b} V dx = \frac{5}{64}\frac{\pi\gamma\sqrt{g}}{c_f} A^{3/2} \sin 2\alpha_b, [m/s]$$

where :

π	=	3.142	[dimensionless]
g	=	9.81	[m/s^2]
c_f	=	0.005	[dimensionless]

and :

$$A = \frac{9}{4}\left(\frac{w^2}{g}\right)^{1/3}, [m^{1/3}]$$

For these experimental cases, the grain sizes were different. Therefore, the fall velocity *w* and *A* will be varied, however, the temperature is still assumed as 15 deg.

[C] Calculation of the Wave Energy Flux *F* :

$$F = \frac{1}{8}\rho g H_b^2 C_{gb} \cos\alpha_b, [Nm/m^2]$$

where :

ρ	=	1025	[kg/m^3]
g	=	9.81	[m/s^2]

[D] Calculation of the Total Longshore Sediment Transport Rate K or Q/ε :

The newly derived formula :

$$Q = \frac{\varepsilon}{(\rho_s - \rho)(1-a)gw} FV, [m^3/s]$$

where :

ρ	=	1025	[kg/m^3]
g	=	9.81	[m/s^2]
ρ_s	=	2650	[kg/m^3]
a	=	0.4	[dimensionless]

and :

$$\text{Const} = \frac{1}{(\rho_s - \rho)(1-a)g} = 0.0001046$$

The result is,

		[A]						[B]		[C]	[D]		
Site	H_b [m]	C_{gb} [m/s]	d_{50} [mm]	w [m/s]	A [$m^{1/3}$]	α_b [deg]	$\sin 2\alpha_b$ [-]	V_m [m/s]	$\cos \alpha_b$	F [Nm/m^2]	K or Q/e [m^3/s]	$Q_{measured}$ [m^3/s]	$\varepsilon = Q_{measured}/K$ [-]
El Moreno	0.45	*2.3790*	0.6	0.07970	0.1947	10	0.3420	*3.5242*	0.9848	*596.3110*	*2.7568*	0.00471	*0.001709*
El Moreno	0.56	*2.6539*	0.6	0.07970	0.1947	14	0.4695	*4.8375*	0.9703	*1014.9959*	*6.4410*	0.00882	*0.001369*
El Moreno	0.39	*2.2147*	0.6	0.07970	0.1947	9.6	0.3289	*3.3887*	0.9860	*417.4714*	*1.8558*	0.00153	*0.000824*
El Moreno	0.51	*2.5326*	0.6	0.07970	0.1947	10.9	0.3714	*3.8266*	0.9995	*827.5166*	*4.1540*	0.00447	*0.001076*
El Moreno	0.4	*2.2429*	0.6	0.07970	0.1947	2.5	0.0872	*0.8981*	0.9990	*450.6367*	*0.5309*	0.00064	*0.001206*
El Moreno	0.41	*2.2708*	0.6	0.07970	0.1947	7.4	0.2554	*2.6322*	0.9917	*475.7923*	*1.6428*	0.00094	*0.000572*

El Moreno	0.4	*2.2429*	0.6	0.07970	0.1947	4	0.1392	*1.4341*	0.9976	*449.9672*	*0.8465*	0.00217	*0.002564*
Silver Strand	1.27	*3.9966*	0.175	0.02166	0.0817	0.3	0.0105	*0.0293*	1.0000	*8102.0224*	*0.3117*	0.00134	*0.004299*
Silver Strand	1.46	*4.2851*	0.175	0.02166	0.0817	4.4	0.1530	*0.4284*	0.9971	*11446.9652*	*6.4333*	0.03155	*0.004904*
Silver Strand	0.75	*3.0713*	0.175	0.02166	0.0817	5.8	0.2011	*0.5631*	0.9949	*2160.3009*	*1.5958*	0.00492	*0.003083*
Silver Strand	0.8	*3.1720*	0.175	0.02166	0.0817	4.3	0.1495	*0.4188*	0.9972	*2544.4320*	*1.3977*	0.00396	*0.002833*
Leadbetter	0.7	*2.9671*	0.22	0.02786	0.0966	4.2	0.1461	*0.5262*	0.9973	*1822.4991*	*1.2579*	0.00804	*0.006391*
Leadbetter	0.85	*3.2696*	0.22	0.02786	0.0966	3.2	0.1115	*0.4015*	0.9984	*2964.5563*	*1.5613*	0.01498	*0.009594*
Leadbetter	0.78	*3.1321*	0.22	0.02786	0.0966	5.6	0.1942	*0.6996*	0.9952	*2383.6853*	*2.1876*	0.01122	*0.005129*
Leadbetter	1.77	*4.7182*	0.22	0.02786	0.0966	8	0.2756	*0.9928*	0.9903	*18398.2294*	*23.9608*	0.12553	*0.005239*
Leadbetter	0.76	*3.0917*	0.22	0.02786	0.0966	3.8	0.1323	*0.4764*	0.9978	*2239.5884*	*1.3995*	0.00228	*0.001629*
Leadbetter	0.65	*2.8592*	0.22	0.02786	0.0966	6.2	0.2147	*0.7734*	0.9942	*1509.5202*	*1.5315*	0.00318	*0.002076*
Leadbetter	0.69	*2.9459*	0.22	0.02786	0.0966	5.7	0.1977	*0.7119*	0.9951	*1754.1234*	*1.6382*	0.00797	*0.004865*
Leadbetter	0.75	*3.0713*	0.22	0.02786	0.0966	5.9	0.2045	*0.7366*	0.9947	*2159.9147*	*2.0869*	0.00775	*0.003714*
Torrey Pines	1.12	*3.7532*	0.2	0.02508	0.0901	3.4	0.1184	*0.3840*	0.9982	*5907.0417*	*2.9757*	0.01567	*0.005266*
Torrey Pines	1.29	*4.0279*	0.157	0.01992	0.0773	3.4	0.1184	*0.3050*	0.9982	*8410.0632*	*3.3647*	0.0375	*0.011145*
Duck	1.99	*5.0028*	0.46	0.06270	0.1659	16.5	0.5446	*4.4153*	0.9588	*23875.8995*	*138.2895*	0.262	*0.001895*
Duck	0.88	*3.3268*	0.46	0.06270	0.1659	5	0.1736	*1.4077*	0.9962	*3225.8264*	*5.9571*	0.0045	*0.000755*
Lake Worth	0.55	*2.6301*	0.42	0.05673	0.1552	16.8	0.5534	*4.0591*	0.9573	*957.3125*	*5.0974*	0.00308	*0.000604*
Lake Worth	0.46	*2.4053*	0.42	0.05673	0.1552	11.5	0.3907	*2.8660*	0.9799	*626.8698*	*2.3568*	0.00243	*0.001031*
Lake Worth	0.28	*1.8766*	0.42	0.05673	0.1552	15.5	0.5150	*3.7778*	0.9636	*178.1951*	*0.8831*	0.00086	*0.000974*
Channel Islands	0.84	*3.2503*	0.22	0.02786	0.0966	3.1	0.1080	*0.3890*	0.9985	*2878.4078*	*1.4688*	0.0151	*0.010281*
Channel Islands	1.09	*3.7025*	0.22	0.02786	0.0966	3.1	0.1080	*0.3890*	0.9985	*5521.0331*	*2.8173*	0.01789	*0.006350*
Channel Islands	1.27	*3.9966*	0.22	0.02786	0.0966	3	0.1045	*0.3765*	0.9986	*8091.0297*	*3.9960*	0.04589	*0.011484*
Channel Islands	1.27	*3.9966*	0.22	0.02786	0.0966	3.2	0.1115	*0.4015*	0.9984	*8089.5003*	*4.2605*	0.04193	*0.009842*
Channel Islands	1.14	*3.7865*	0.22	0.02786	0.0966	3.1	0.1080	*0.3890*	0.9985	*6176.1272*	*3.1515*	0.02568	*0.008148*
Channel Islands	1.67	*4.5830*	0.22	0.02786	0.0966	2.8	0.0976	*0.3515*	0.9988	*16045.8404*	*7.3981*	0.03407	*0.004605*
Price Inlet	0.85	*3.2696*	0.25	0.03206	0.1061	9	0.3090	*1.2810*	0.9877	*2932.6304*	*12.2507*	0.00731	*0.000597*
Price Inlet	0.92	*3.4016*	0.25	0.03206	0.1061	4	0.1392	*0.5769*	0.9976	*3609.9438*	*6.7917*	0.00255	*0.000375*
Price Inlet	0.79	*3.1521*	0.18	0.02234	0.0834	5	0.1736	*0.5016*	0.9962	*2463.2141*	*4.0288*	0.00688	*0.001708*
Price Inlet	0.99	*3.5286*	0.18	0.02234	0.0834	9	0.3090	*0.8926*	0.9877	*4293.3669*	*12.4963*	0.0146	*0.001168*
Pointe Sapin	1	*3.5464*	0.58	0.07678	0.1899	9.3	0.3190	*3.1663*	0.9869	*4398.8966*	*45.4189*	0.0463	*0.001019*
Pointe Sapin	0.74	*3.0507*	0.58	0.07678	0.1899	10.9	0.3714	*3.6866*	0.9820	*2061.8763*	*24.7870*	0.01768	*0.000713*

Anaheim Bay	0.494	*2.4926*	0.4	0.05377	0.1498	21	0.6691	*4.6516*	0.9336	*713.7715*	*10.8268*	0.01051	*0.000971*
Anaheim Bay	1.026	*3.5922*	0.4	0.05377	0.1498	9	0.3090	*2.1482*	0.9877	*4694.3819*	*32.8844*	0.01913	*0.000582*
Anaheim Bay	0.338	*2.0618*	0.4	0.05377	0.1498	21	0.6691	*4.6516*	0.9336	*276.3972*	*4.1925*	0.00273	*0.000651*
Anaheim Bay	0.654	*2.8680*	0.4	0.05377	0.1498	21	0.6691	*4.6516*	0.9336	*1439.4156*	*21.8337*	0.00556	*0.000255*
Anaheim Bay	0.612	*2.7744*	0.4	0.05377	0.1498	21	0.6691	*4.6516*	0.9336	*1219.3275*	*18.4953*	0.01508	*0.000815*
Pt. Mugu	1.1	*3.7195*	0.154	0.01882	0.0744	15	0.5000	*1.2166*	0.9659	*5464.0615*	*21.6767*	0.007716	*0.000356*
Lake Michigan	0.254	*1.7873*	0.5	0.06873	0.1764	12	0.4067	*3.6141*	0.9781	*141.7682*	*1.6708*	0.00304	*0.001820*
Lake Michigan	0.356	*2.1160*	0.5	0.06873	0.1764	10	0.3420	*3.0390*	0.9848	*331.9453*	*3.2896*	0.0024	*0.000730*
Lake Michigan	0.28	*1.8766*	0.43	0.05822	0.1579	13	0.4384	*3.2998*	0.9744	*180.1810*	*1.9388*	0.00206	*0.001063*
Lake Michigan	0.585	*2.7125*	0.5	0.06873	0.1764	5	0.1736	*1.5430*	0.9962	*1162.3157*	*5.8481*	0.0022	*0.000376*
Lake Michigan	0.204	*1.6018*	0.23	0.02925	0.0998	16	0.5299	*2.0043*	0.9613	*80.5392*	*0.5264*	0.00116	*0.002204*
Lake Michigan	0.176	*1.4878*	0.285	0.03703	0.1168	6	0.2079	*0.9955*	0.9945	*57.6084*	*0.1870*	0.00019	*0.001016*
Lake Michigan	0.076	*0.9777*	0.32	0.04207	0.1272	27	0.8090	*4.4001*	0.8910	*6.3242*	*0.0907*	0.00028	*0.003086*
Cape Thompson	1.676	*4.5912*	1	0.13337	0.2744	25	0.7660	*13.2081*	0.9063	*14690.9823*	*632.7461*	0.04212	*0.000067*
Cotonou	1.4	*4.1962*	0.4	0.05377	0.1498	9	0.3090	*2.1482*	0.9877	*10210.1025*	*71.5224*	0.03858	*0.000539*
Safi (Maroc)	3.4	*6.5392*	0.5	0.06873	0.1764	10.4	0.3551	*3.1553*	0.9836	*93453.0083*	*961.5525*	0.4756	*0.000495*
Agadir (")	2.1	*5.1392*	0.17	0.02098	0.0800	4.2	0.1461	*0.3962*	0.9973	*28409.9486*	*36.7087*	0.1096	*0.002986*
Agadir (")	3	*6.1425*	0.2	0.02508	0.0901	5	0.1736	*0.5632*	0.9962	*69220.9530*	*127.1269*	0.13699	*0.001078*
Pt. Noire	1.9	*4.8884*	0.3	0.03918	0.1213	1.9	0.0663	*0.3358*	0.9995	*22168.4463*	*24.2711*	0.01929	*0.000795*
Lome (Benin)	1.6	*4.4859*	0.19	0.02371	0.0868	4.9	0.1702	*0.5218*	0.9963	*14381.3587*	*24.4687*	0.04019	*0.001643*
Ventnor	0.45	*2.3790*	0.2	0.02508	0.0901	6.4	0.2215	*0.7186*	0.9938	*601.7365*	*1.4100*	0.00386	*0.002738*
Nags Head	0.6	*2.7470*	0.29	0.03775	0.1183	6.4	0.2215	*1.0813*	0.9938	*1235.2452*	*4.3555*	0.0135	*0.003100*
Ivory Coast	3	*6.1425*	0.5	0.06873	0.1764	4.5	0.1564	*1.3900*	0.9969	*69271.1459*	*313.9824*	0.03215	*0.000102*
DUCK	0.52	*2.5573*	0.2	0.02508	0.0901	6.5	0.2250	*0.7296*	0.9936	*863.5704*	*2.0545*	0.00119	*0.000579*
DUCK	0.52	*2.5573*	0.2	0.02508	0.0901	6.5	0.2250	*0.7296*	0.9936	*863.5704*	*2.0545*	0.00145	*0.000706*
DUCK	0.6	*2.7470*	0.193	0.02289	0.0848	5.5	0.1908	*0.5647*	0.9954	*1237.2692*	*2.2784*	0.00206	*0.000904*
DUCK	0.6	*2.7470*	0.193	0.02289	0.0848	5.5	0.1908	*0.5647*	0.9954	*1237.2692*	*2.2784*	0.00254	*0.001115*
DUCK	0.45	*2.3790*	0.84	0.11540	0.2492	5.5	0.1908	*2.8467*	0.9954	*602.7224*	*5.5949*	0.00379	*0.000677*
DUCK	0.45	*2.3790*	0.84	0.11540	0.2492	5.5	0.1908	*2.8467*	0.9954	*602.7224*	*5.5949*	0.00559	*0.000999*
Miyazu	0.058	*0.8541*	0.32	0.04207	0.1272	5	0.1736	*0.9444*	0.9962	*3.5975*	*0.0111*	2.30E-05	*0.002076*
Miyazu	0.064	*0.8972*	0.32	0.04207	0.1272	5	0.1736	*0.9444*	0.9962	*4.6013*	*0.0142*	1.90E-05	*0.001341*
Miyazu	0.073	*0.9582*	0.32	0.04207	0.1272	5	0.1736	*0.9444*	0.9962	*6.3935*	*0.0197*	2.90E-05	*0.001473*

Miyazu	0.148	*1.3643*	0.32	0.04207	0.1272	5	0.1736	*0.9444*	0.9962	*37.4187*	*0.1152*	3.20E-05	*0.000278*
Miyazu	0.193	*1.5580*	0.32	0.04207	0.1272	5	0.1736	*0.9444*	0.9962	*72.6654*	*0.2238*	3.90E-05	*0.000174*
Miyazu	0.351	*2.1011*	0.32	0.04207	0.1272	5	0.1736	*0.9444*	0.9962	*324.1173*	*0.9982*	0.00028	*0.000281*
Miyazu	0.382	*2.1919*	0.32	0.04207	0.1272	5	0.1736	*0.9444*	0.9962	*400.4911*	*1.2334*	0.00021	*0.000170*
Miyazu	0.442	*2.3578*	0.32	0.04207	0.1272	5	0.1736	*0.9444*	0.9962	*576.7533*	*1.7762*	0.00029	*0.000163*
Rosseika	1.12	*3.7532*	0.35	0.04642	0.1358	12	0.4067	*2.4413*	0.9781	*5788.1468*	*46.0784*	0.00614	*0.000133*
Rosseika	0.84	*3.2503*	0.26	0.03348	0.1092	15	0.8660	*3.7484*	0.9659	*2784.4029*	*34.0344*	0.00089	*0.000026*
Rosseika	0.56	*2.6539*	0.25	0.03206	0.1061	10	0.3420	*1.4179*	0.9848	*1030.1764*	*4.7630*	0.00184	*0.000386*
Rosseika	0.653	*2.8658*	0.25	0.03206	0.1061	15	0.8660	*3.5902*	0.9659	*1483.6000*	*17.3687*	0.0019	*0.000109*
Rosseika	0.933	*3.4255*	0.22	0.02786	0.0966	15	0.8660	*3.1193*	0.9659	*3620.2451*	*36.8236*	0.00361	*0.000098*
Rosseika	0.746	*3.0631*	0.32	0.04207	0.1272	10	0.3420	*1.8602*	0.9848	*2110.0299*	*12.7991*	0.00165	*0.000129*
Rosseika	0.653	*2.8658*	0.36	0.04788	0.1386	10	0.3420	*2.1175*	0.9848	*1512.6014*	*10.4443*	0.00087	*0.000083*
Primorskoe	1.493	*4.3333*	0.43	0.05822	0.1579	30	0.8660	*6.5188*	0.8660	*10514.0549*	*223.4998*	0.02852	*0.000128*
Primorskoe	0.84	*3.2503*	0.4	0.05377	0.1498	15	0.8660	*6.0204*	0.9659	*2784.4029*	*54.6629*	0.00823	*0.000151*
Primorskoe	1.4	*4.1962*	0.39	0.05229	0.1470	10	0.3420	*2.3123*	0.9848	*10180.3248*	*76.7626*	0.01933	*0.000252*
Primorskoe	1.773	*4.7222*	0.33	0.04351	0.1301	25	0.7660	*4.3098*	0.9063	*16909.7676*	*237.6458*	0.05737	*0.000241*
Primorskoe	1.493	*4.3333*	0.34	0.04497	0.1329	18	0.5878	*3.4173*	0.9511	*11546.3823*	*128.6657*	0.02412	*0.000187*
Primorskoe	0.933	*3.4255*	0.25	0.03206	0.1061	10	0.3420	*1.4179*	0.9848	*3691.0137*	*17.0654*	0.00715	*0.000419*
Rosseika	1.586	*4.4662*	0.36	0.04788	0.1386	25	0.7660	*4.7426*	0.9063	*12797.4593*	*197.9154*	0.02795	*0.000141*
Rosseika	0.84	*3.2503*	0.3	0.03918	0.1213	5	0.1736	*0.8797*	0.9962	*2871.6576*	*8.2378*	0.00332	*0.000403*
Rosseika	0.933	*3.4255*	0.36	0.04788	0.1386	25	0.7660	*4.7426*	0.9063	*3396.7995*	*52.5322*	0.00472	*0.000090*
Rosseika	0.746	*3.0631*	0.32	0.04207	0.1272	18	0.5878	*3.1968*	0.9511	*2037.7152*	*21.2423*	0.00433	*0.000204*
Rosseika	0.746	*3.0631*	0.28	0.03632	0.1153	20	0.6428	*3.0185*	0.9397	*2013.3671*	*19.8173*	0.0059	*0.000298*
Rosseika	0.933	*3.4255*	0.3	0.03918	0.1213	10	0.3420	*1.7327*	0.9848	*3691.0137*	*20.8549*	0.0048	*0.000230*
Rosseika	1.12	*3.7532*	0.28	0.03632	0.1153	5	0.1736	*0.8154*	0.9962	*5894.9414*	*15.6749*	0.00246	*0.000157*
Rosseika	0.84	*3.2503*	0.4	0.05377	0.1498	5	0.1736	*1.2072*	0.9962	*2871.6576*	*11.3040*	0.00099	*0.000088*
Rosseika	1.12	*3.7532*	0.37	0.04935	0.1414	5	0.1736	*1.1080*	0.9962	*5894.9414*	*21.2980*	0.00121	*0.000057*
Rosseika	1.493	*4.3333*	0.28	0.03632	0.1153	20	0.6428	*3.0185*	0.9397	*11408.4180*	*112.2916*	0.0342	*0.000305*
Rosseika	1.12	*3.7532*	0.28	0.03632	0.1153	30	0.8660	*4.0668*	0.8660	*5124.6685*	*67.9596*	0.01908	*0.000281*
Rosseika	0.746	*3.0631*	0.29	0.03775	0.1183	5	0.1736	*0.8475*	0.9962	*2134.4280*	*5.8989*	0.00129	*0.000219*
Rosseika	0.933	*3.4255*	0.32	0.04207	0.1272	10	0.3420	*1.8602*	0.9848	*3691.0137*	*22.3891*	0.00288	*0.000129*
Kinburn	1.4	*4.1962*	0.55	0.07243	0.1827	30	0.8660	*8.1093*	0.8660	*8952.4274*	*236.7333*	0.05047	*0.000213*

Kinburn	0.746	*3.0631*	0.7	0.09443	0.2180	35	0.9397	*11.4719*	0.8192	*1755.1635*	*65.6582*	0.00335	*0.000051*
Kinburn	0.56	*2.6539*	0.3	0.03918	0.1213	10	0.3420	*1.7327*	0.9848	*1030.1764*	*5.8207*	0.0026	*0.000447*
Kinburn	0.653	*2.8658*	0.28	0.03632	0.1153	20	0.6428	*3.0185*	0.9397	*1443.3075*	*14.2063*	0.00113	*0.000080*
Kinburn	0.933	*3.4255*	0.48	0.06571	0.1712	15	0.8660	*7.3572*	0.9659	*3620.2451*	*86.8538*	0.00201	*0.000023*
Kinburn	0.746	*3.0631*	0.5	0.06873	0.1764	15	0.8660	*7.6951*	0.9659	*2069.5739*	*51.9316*	0.00112	*0.000022*
Kinburn	0.56	*2.6539*	0.47	0.06420	0.1686	10	0.3420	*2.8391*	0.9848	*1030.1764*	*9.5373*	0.00045	*0.000047*
Kinburn	0.746	*3.0631*	0.28	0.03632	0.1153	10	0.3420	*1.6061*	0.9848	*2110.0299*	*11.0508*	0.00126	*0.000114*
Kinburn	1.306	*4.0528*	0.32	0.04207	0.1272	10	0.3420	*1.8602*	0.9848	*8556.5657*	*51.9028*	0.01212	*0.000234*
Kinburn	1.773	*4.7222*	0.23	0.02925	0.0998	20	0.6428	*2.4312*	0.9397	*17532.6573*	*138.9975*	0.05252	*0.000378*
Kinburn	0.653	*2.8658*	0.24	0.03065	0.1030	20	0.6428	*2.5477*	0.9397	*1443.3075*	*11.9908*	0.00145	*0.000121*
Kinburn	0.84	*3.2503*	0.22	0.02786	0.0966	30	0.8660	*3.1193*	0.8660	*2496.4274*	*25.3926*	0.00983	*0.000387*
Kinburn	1.306	*4.0528*	0.23	0.02925	0.0998	25	0.7660	*2.8974*	0.9063	*7874.5137*	*74.3994*	0.02712	*0.000365*
Shoreham	0.31	*1.9745*	0.15	0.01828	0.0730	12.5	0.4226	*0.9989*	0.9763	*232.8498*	*0.7585*	4.80E-05	*0.000063*
Shoreham	0.33	*2.0372*	0.15	0.01828	0.0730	13	0.4387	*1.0370*	0.9744	*271.7058*	*0.9188*	6.10E-05	*0.000066*
Shoreham	0.37	*2.1572*	0.15	0.01828	0.0730	18.5	0.6018	*1.4225*	0.9483	*352.0067*	*1.6328*	0.0003	*0.000184*
Shoreham	0.45	*2.3790*	0.15	0.01828	0.0730	20	0.6428	*1.5193*	0.9397	*568.9933*	*2.8189*	0.00024	*0.000085*
Shoreham	0.33	*2.0372*	0.15	0.01828	0.0730	13	0.4384	*1.0361*	0.9744	*271.7058*	*0.9180*	7.00E-05	*0.000076*
Shoreham	0.6	*2.7470*	0.15	0.01828	0.0730	14	0.4695	*1.1096*	0.9703	*1206.0695*	*4.3641*	0.00038	*0.000087*
Shoreham	0.9	*3.3644*	0.15	0.01828	0.0730	9	0.3090	*0.7304*	0.9877	*3383.1113*	*8.0577*	0.00028	*0.000035*
Portugal	1.2	*3.8849*	0.38	0.05082	0.1442	10	0.3420	*2.2472*	0.9848	*6924.5995*	*50.7428*	0.00675	*0.000133*
Lobito	0.65	*2.8592*	0.45	0.06121	0.1633	25	0.7660	*6.0619*	0.9063	*1376.0975*	*27.2017*	0.00643	*0.000236*
											Mean		**0.001527048**
											Standard deviation		**0.002412056**

B.6 Field Database : Longshore Sediment Transport by Wang *et at.,* 1998.

[A] Calculation of the Group Velocity C_{gb} :

$$C_{gb} = \sqrt{g \frac{H_b}{\gamma}}, [m/s]$$

where :

g	=	9.81	[m/s^2]
γ	=	0.78	[dimensionless]

Since there was no information about breaker index γ, the value of 0.78 is used.

[B] Calculation of the Average Longshore Current V_m :

$$V_m = \frac{1}{x_b} \int_0^{x_b} V dx = \frac{5}{64} \frac{\pi \gamma \sqrt{g}}{c_f} A^{3/2} \sin 2\alpha_b, [m/s]$$

where :

π	=	3.142	[dimensionless]
g	=	9.81	[m/s^2]
c_f	=	0.005	[dimensionless]
γ	=	0.78	[dimensionless]

and :

$$A = \frac{9}{4} \left(\frac{w^2}{g} \right)^{1/3}, [m^{1/3}]$$

In these experiments, the grain sizes d_{50} were different. Therefore, the fall velocity w and A will be varied, however, the temperature is still assumed as 15 deg.

[C] Calculation of the Wave Energy Flux F :

$$F = \frac{1}{8}\rho g H_b^2 C_{gb} \cos\alpha_b, [Nm/m^2]$$

where :

ρ	=	1025	[kg/m^3]
g	=	9.81	[m/s^2]

[D] Calculation of the Total Longshore Sediment Transport Rate K or Q/ε :

The newly derived formula :

$$Q = \frac{\varepsilon}{(\rho_s - \rho)(1-a)gw} FV, [m^3/s]$$

where :

ρ	=	1025	[kg/m^3]
g	=	9.81	[m/s^2]
ρ_s	=	2650	[kg/m^3]
a	=	0.4	[dimensionless]

and :

$$\text{Const} = \frac{1}{(\rho_s - \rho)(1-a)g} = 0.0001046$$

The result is,

Location	H_{rms} [m]	[A] C_{gb} [m/s]	d_{50} [mm]	w [m/s]	A [$m^{1/3}$]	α_b [deg]	$\sin 2\alpha_b$ [-]	[B] V_m [m/s]	$\cos \alpha_b$ [-]	[C] F [Nm/m^2]	[D] K or Q/e [m^3/s]	$Q_{measured}$ [m^3/s]	$\varepsilon = Q_{measured}/K$ [-]
Emerald Isle, NC	0.79	*3.1521*	0.35	0.0441	0.1311	13.5	0.4540	*2.5858*	0.9724	*2404.3037*	*14.7551*	0.003537	*0.00024*
Onslow Beach, NC	0.61	*2.7698*	2.25	0.2001	0.3596	12	0.4067	*10.5190*	0.9781	*1267.1239*	*6.9658*	0.00135	*0.000194*
Myrtle Beach, SC	0.51	*2.5326*	0.26	0.0318	0.1055	4	0.1392	*0.5716*	0.9976	*825.9549*	*1.5539*	0.000193	*0.000124*
Jekyll Island, GA	0.2	*1.5860*	0.17	0.0199	0.0772	3	0.1045	*0.2691*	0.9986	*79.6287*	*0.1125*	6.43E-05	*0.000571*
Jekyll Island, GA	0.35	*2.0981*	0.26	0.0318	0.1055	10	0.3420	*1.4048*	0.9848	*318.1352*	*1.4709*	0.001672	*0.001137*
Anastacia Beach, FL	0.49	*2.4825*	0.19	0.0225	0.0838	5.5	0.1908	*0.5550*	0.9954	*745.7208*	*1.9236*	0.000257	*0.000134*
N. Mantazas Beach, FL	0.44	*2.3524*	0.28	0.0345	0.1113	7.2	0.2487	*1.1082*	0.9921	*567.9154*	*1.9092*	0.000386	*0.000202*
Canaveral Seashore, FL	0.46	*2.4053*	0.9	0.1245	0.2621	9	0.3090	*4.9737*	0.9877	*631.8363*	*2.6391*	0.000611	*0.000232*
Melbourne Beach, FL	0.5	*2.5077*	1.5	0.1633	0.3141	2.5	0.0872	*1.8404*	0.9990	*787.2298*	*0.9274*	0.000193	*0.000208*
Beverly Beach, FL	0.36	*2.1278*	0.41	0.0524	0.1473	11.5	0.3907	*2.6485*	0.9799	*339.6558*	*1.7940*	0.000322	*0.000179*
Lido Key Beach, FL	0.38	*2.1861*	0.68	0.0915	0.2134	14	0.4695	*5.5515*	0.9703	*384.9933*	*2.4431*	0.001254	*0.000513*
Lido Key Beach, FL	0.34	*2.0679*	0.54	0.0710	0.1802	19	0.6157	*5.6497*	0.9455	*284.0910*	*2.3642*	0.00119	*0.000503*
Lido Key Beach, FL	0.21	*1.6252*	0.37	0.0468	0.1366	2.6	0.0906	*0.5488*	0.9990	*89.9893*	*0.1103*	3.22E-05	*0.000292*
St. George Island, FL	0.29	*1.9098*	0.29	0.0358	0.1142	35.3	0.9432	*4.3685*	0.8161	*164.7587*	*2.1008*	0.001447	*0.000689*
St. George Island, FL	0.22	*1.6634*	0.41	0.0524	0.1473	31.5	0.8910	*6.0396*	0.8526	*86.2805*	*1.0392*	9.65E-05	*9.29E-05*

St. George Island, FL	0.28	*1.8766*	0.43	0.0552	0.1525	23	0.7719	*5.5139*	0.9205	*170.2203*	*1.7762*	0.000193	*0.000109*
St. Joseph Island, FL	0.53	*2.5818*	0.24	0.0291	0.0994	9.3	0.3190	*1.1997*	0.9869	*899.5668*	*3.8788*	0.0018	*0.000464*
Grayton Beach, FL	0.56	*2.6539*	0.28	0.0345	0.1113	8.5	0.2924	*1.3028*	0.9890	*1034.5784*	*4.0890*	0.001929	*0.000472*
Redington Beach, FL	0.36	*2.1278*	0.85	0.1169	0.2514	8.4	0.2890	*4.3686*	0.9893	*342.8958*	*1.3396*	0.000482	*0.00036*
Redington Beach, FL	0.28	*1.8766*	0.2	0.0238	0.0870	10.7	0.3649	*1.1230*	0.9826	*181.7053*	*0.8963*	0.000193	*0.000215*
Redington Beach, FL	0.32	*2.0061*	0.9	0.1245	0.2621	19.2	0.6211	*9.9975*	0.9444	*243.8429*	*2.0472*	0.000257	*0.000126*
Redington Beach, FL	0.24	*1.7374*	0.43	0.0552	0.1525	15.8	0.5240	*3.7428*	0.9622	*121.0296*	*0.8573*	0.000161	*0.000188*
Redington Beach, FL	0.69	*2.9459*	0.37	0.0468	0.1366	13.1	0.4415	*2.6732*	0.9740	*1716.9635*	*10.2471*	0.004662	*0.000455*
Indian Shores, FL	0.36	*2.1278*	0.32	0.0399	0.1228	20	0.4628	*2.3885*	0.9397	*325.7108*	*2.0376*	0.001093	*0.000536*
Indian Shores, FL	0.31	*1.9745*	0.4	0.0510	0.1446	1.8	0.0628	*0.4142*	0.9995	*238.3856*	*0.2023*	3.22E-05	*0.000159*
Indian Rocks Beach, FL	0.36	*2.1278*	0.28	0.0345	0.1113	7.7	0.2656	*1.1834*	0.9910	*343.4888*	*1.2331*	0.000611	*0.000496*
Indian Rocks Beach, FL	0.34	*2.0679*	0.42	0.0538	0.1499	7.5	0.2588	*1.8015*	0.9914	*297.8900*	*1.0422*	0.000739	*0.000709*
Indian Rocks Beach, FL	0.19	*1.5458*	1.38	0.1567	0.3055	10	0.3420	*6.9274*	0.9848	*69.0757*	*0.3193*	9.65E-05	*0.000302*
Indian Rocks Beach, FL	0.14	*1.3269*	1.29	0.1515	0.2987	8.2	0.0282	*0.5529*	0.9898	*32.3554*	*0.0123*	6.43E-05	*0.005208*

Mean	**0.000521**
Standard deviation	**0.000915**